Master Thesis

Rafael van Loon

Design and validation of a modular laparoscope for low-income countries

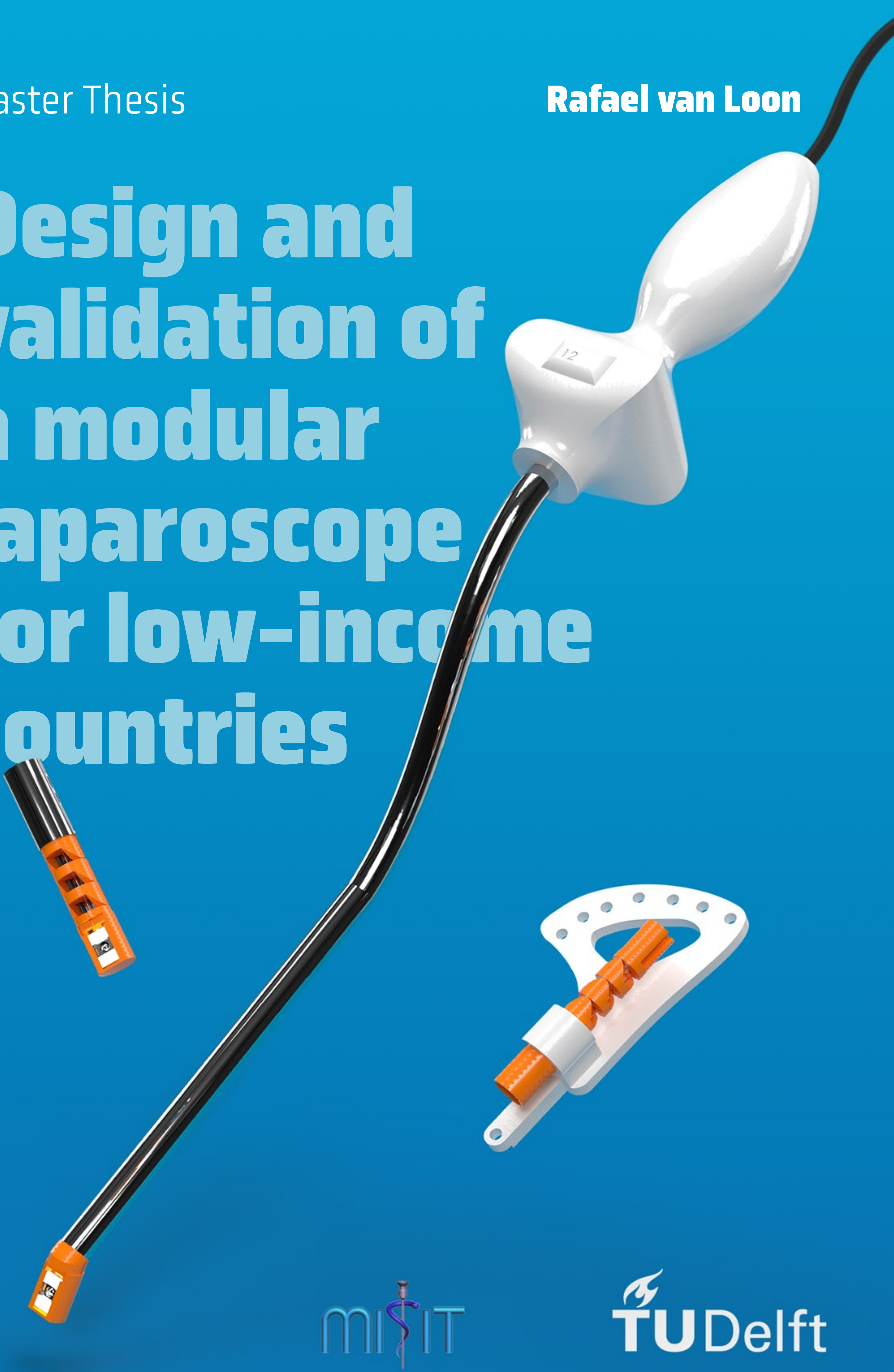

MISIT

TU Delft

Master Thesis

By

Rafael van Loon

To obtain the degree of Master of Science

At the Delft University of Technology

To be defended publicly on the 12th of February 2024

Student number: 5183464

Project duration: May 2023 - February 2024

Thesis committee: Prof. Dr. J. Dankelman, TU Delft, Chair

Dr. Ir. T. Horeman, TU delft

A digital copy of this thesis is available at: *https://repository.tudelft.nl/*

Preface

I want to express my gratitude to Jenny Dankelman and Roos Oosting for the guidance, opportunities, and support throughout this project. Making it possible for me to graduate in the field of laparoscopy and come in contact with so many experts from this field to help me along the way. Special thanks to Paul Bons from the BovenIJ Hospital in Amsterdam for enabling me to measure image quality metrics with their laparoscopes. Additionally, I would like to thank Dr. J. Gnanaraj for his involvement in the project to hear and see what laparoscopic surgeons need and want in a low-cost laparoscope. Also, I would like to thank Robert den Butter for his help in setting up the measurement setup for the first part of this thesis and his general support and friendship during the project. Lastly, I would like to thank my loved ones around me (Giorgia Girelli, Wim van Loon, Lia Oegema) who helped in any way possible to succeed in the sometimes stressful periods.

Rafael van Loon
Rotterdam, Januari 2024

Abstract

In laparoscopic surgery, the goal of the surgeon is to decrease the procedure's invasiveness. These techniques have been a great addition to modern medicine, reducing the invasiveness of abdominal surgeries. The patient has a decreased chance of infection, blood loss, and reduced post-operative pain. Which results in shorter hospital stays and greatly improved recovery times.

Laparoscopy has been widely adopted in the Western world, though it is found less often in less developed countries. These countries could be more significant beneficiaries of these techniques than Western countries, where there are clean water, blood banks, and sick leave agreements. The reason for the reduced adoption of this method of surgery is related to the inherent cost of performing laparoscopic surgery. The equipment and instruments used are large, fragile, and costly, especially the imaging system, which can cost up to 50,000 dollars and, therefore, not accessible in low-resource settings.

In these lower resource settings, these technologies could also be an excellent alternative for diagnostics of the abdomen. The cost of laparoscopic diagnostics equipment compared to ultrasound, CT, and MRI is 1:500:2500:4500. This might explain why 1/3 of all laparoscopic surgeries are already diagnostic in regions in Africa, but this is not available to most. The remoteness of areas and the initial cost make it infeasible to perform this diagnostic and general laparoscopic surgery on those who would benefit the most from it. The problem of not being able to perform proper diagnostics is seen as the main reason for the ten times higher rate of preoperative deaths found in low-income countries than in Western countries.

Research projects have been set up to tackle the size problems, fragility, and cost to create mobile, low-cost laparoscopes that could be used for laparoscopic surgery in low-income countries and rural settings. The problem with these Low-cost laparoscopes is that the scopes don't produce enough light, have low resolution, and are designed for specific use cases where the scope can look straight at the tissue. However, a laparoscope, which looks straight at tissue and is often called 0 degrees scope, can't be used for most procedures and diagnostics interventions. Commercial laparoscopes often use a 30-degree lens offset to move around tissue and position the camera differently without creating new incisions.

This thesis will tackle the problem of designing and validating a laparoscope that solves the issues with low-cost laparoscopes found in academia. The imaging system analysis and design and validation of the laparoscope are split into two parts, the first being a comparative analysis of low-cost imaging systems and commercial laparoscopes found in Western hospitals. To find a low-cost imaging system comparable to the state-of-the-art of about ten years ago and that can be integrated into a laparoscope. The second part covers the design and evaluation of the laparoscope based on the “Roadmap for the Design of Surgical Equipment for Safe Surgery Worldwide.” The roadmaps analysis based on literature and end-user input resulted in an extensive list of requirements for the design of a laparoscope for low-income settings in sub-Saharan Africa and India. The designed laparoscope is modular and can facilitate gas and gasless laparoscopy with the change of minor components. Tests on its requirements and a user test by a laparoscopic surgeon have validated the laparoscope function and requirements and exposed potential improvements. The laparoscopic surgeon expressed the significant impact the modular laparoscope could have on laparoscopy in low-income countries and rural settings.

Index terms: Laparoscopic surgery, Biomedical device, LMICs, Global surgery

Table of Contents

Part 1: Analysis of imaging systems for the design of a low-cost laparoscope

Autor: Rafael van Loon

Thesis committee: Prof. Dr. J. Dankelman, TU Delft, Chair

Dr. Ir. T. Horeman, TU delft

Comparative Analysis of Low-Cost Imaging Systems versus Commercial Laparoscopes

Abstract- **Laparoscopy surgery, an effective and less invasive method for abdominal operations, is often costly due to specialized equipment and training requirements. The procedure involves small incisions for inserting equipment, including a camera system with slender optical lenses, to illuminate and visualize internal tissues. These imaging systems, including processors, are often large, fragile, and expensive, often exceeding $25,000. Recent research has explored using low-cost, off-the-shelf components to develop affordable laparoscopes for resource-limited settings. However, these designs often compromise on image quality and optical performance. This paper evaluates two low-cost smartphone-based (Sony IMX 258 and OmniVision 5693) and one low-cost endoscope (OmniVision 9734) USB imaging systems as potential components for a low-cost laparoscope. These are compared to two commercial laparoscopes (Stryker 1688 and Olympus OTV V7) used in the Bovenij hospital in Amsterdam. The assessment of the imaging systems involved a test setup with imaging test charts, analyzed in Imatest based on lenses, image sensors, and processing properties. The Field of View (FOV), Sharpness, Color accuracy, Tone and Noise, Image distortion, and the impact of image-displaying software on image quality were separately investigated using a selection of metrics to compare the imaging systems. The study found that the disparity in image quality between the low-cost smartphone-based imaging systems and commercial systems was smaller than anticipated. The OV5693-based system emerged as the most promising imaging system, offering a larger FOV, comparable sharpness, and superior tone and noise reproduction. It suggests its potential as a viable component in affordable laparoscopic systems, particularly in low-resource settings. Future work should address the limitations, including the impact of external factors like blood and smoke during surgery, and further optimize software for image display. This research contributes to the broader effort of developing a low-cost laparoscope, as detailed in part two of this thesis, "Design and Development of a Modular 500-dollar Laparoscope Using a Low-Cost Imaging System".**

1.1: Introduction:

1.1.1: Overview of laparoscopy for Low-income settings

In minimally invasive surgery (MIS), laparoscopy has emerged as a field of ongoing progress, offering patients reduced recovery times, minimized post-operative discomfort, and lesser surgical scarring[1, 2]. Central to the efficacy of this surgical method is the laparoscope, a specialized instrument equipped with a camera that provides surgeons with an internal view of the abdomen, eliminating the need to open the whole abdomen [3, 4]. However, the initial cost is a significant barrier to the broader adoption of laparoscopy, particularly in resource-limited settings [3, 5, 6].

The design of more affordable imaging devices for lower-income regions has been a topic for research in and outside the laparoscopy field. Projects such as the ready view laparoscope developed by Duke University[7] and other projects or the laryngoscope developed by Lyco Medical, a university project spin-off, have shown great potential. Unlike commercial systems, these projects and other laparoscopic projects [8, 9, 10] use off-the-shelf optical and lighting components and try to combine these to form an affordable solution.

1.1.2: Low-cost image sensors

The image sensor's performance is crucial in determining the device's effectiveness. For designing a device comparable to commercial surgical imaging systems, it's essential to have prior knowledge of the performance and cost-effectiveness of off-the-shelf components. In the case of laparoscopy, the low-cost system should be compared to actual laparoscopes to select the sensor that closely resembles the image quality of commercial laparoscopes.

Choosing a suitable imaging system for a laparoscope depended on three key factors: availability, integrability, and cost. The availability refers to the consistent market presence of components, which excludes options like Raspberry Pi MIPI systems. The integrability considers the size compatibility of the imaging systems. The cost is noted as the direct purchase price of the imaging system and the additional components needed for the illumination and display of the image. Consequently, the most feasible option is a solution with a video output directly converted to a USB JPEG video signal. This decision is evidenced in most low-cost devices, which utilize USB video solutions compatible with laptops [7,8,9].

The sensors that were found when assessing the market are smartphone-based camera sensors with integrated circuitry, which are produced in large volumes for the consumer market. These cameras provide high-resolution imaging at a significantly lower cost due to the economies of scale in smartphone manufacturing [11]. Additionally, there's growing interest in utilizing borescope sensors rebranded as endoscope sensors, commonly used in industrial applications for inspecting pipes and hard-to-reach mechanical components [12]. These two types are the most common types of sensors and come in many different variations.

1.1.3: Comparison of commercial laparoscopes and low-cost imaging systems

This paper covers the objective and subjective comparison of two smartphone and one endoscope imaging systems against two commercial laparoscopes. The first laparoscope, an Olympus OTV V7, was used until a few years ago in the field of urology; the second laparoscope, a Stryker 1688 AIM 4k state-of-the-art 25000-euro imaging system acquired in 2022, used for all types of laparoscopy. The objective and subjective comparison of these imaging systems will cover the Field of View(FOV) sharpness, tone and noise, color, distortions, and the effects of displaying image software.

The low-cost imaging systems are directly sourced from Chinese vendors, making specific claims about their systems that must be validated. So, the Field Of View(FOV) is tested to validate the vendors' claims.

In laparoscopic applications, the efficacy of an image sensor is depending upon its ability to render clear images within the operational range of 40-120mm from the tissue[10,13,24]. Sharpness can be defined and typically tested by the ability to discern detail between contrasting surfaces and the length of pixel transitions between surfaces. In addition, the acutance can be a valuable insight. This subjective metric takes the human eye into the equation and determines how sharp an image is perceived on a certain medium and at a certain distance [28].

Color quality can be examined and split into three parts: color, white balancing, and luminosity accuracy, which are essential to distinguish different types of tissue, to not incidentally to cause damage to other tissue [14].

Distinguishing various shades in tissue imagery is vital for diagnostic accuracy, necessitating a sensor's capability to capture adequate light. This capability is crucial for accurately reproducing exposure and achieving optimal contrast between an image's brightest and darkest parts [15]. Additionally, the sensor's noise and dynamic range performance, which refers to the variation in shade or color within a single tone, are also significant factors in ensuring the diagnostic reliability of the imaging system.

To accurately depict the image on the screen for the surgeon, the image mustn't be too distorted to relate the medical instruments' positions to the position of the tissue[16]. The main perceived distortion is the barrel distortion, though other distortions also play a role.

The final step in laparoscopic imaging involves displaying the image to the surgeon. The image is typically presented directly on a monitor designed for commercial laparoscopes. In this scenario, there is little to no variance in the image quality from processing to display. However, low-cost imaging systems require additional software to project the image onto a computer screen. This additional step can significantly impact the overall image quality, as some software programs are more effectively optimized for image quality and others for low processing load[14].

Goal: This study's objective is to determine the most suitable low-cost imaging system for a laparoscope that closely aligns with the optical and image quality of laparoscopes used in Western hospitals. Additionally, it explores the impact of image-displaying software on the performance of these low-cost systems. The aim is to select the optimal imaging system and display solution for developing an affordable laparoscope. This research feeds into the second part of the thesis, titled "Design and Development of a Modular 500-dollar Laparoscope Using a Low-Cost Imaging System."

1.2: Methods

1.2.1: Tested imaging system and test setup

This study compares a state-of-the-art and a 15-year-old laparoscope used in BovenIJ Hospital, Amsterdam, with low-cost imaging systems for potential use in low-cost laparoscopy. It focuses on evaluating key aspects of these imaging systems. The laparoscopes under assessment, featuring a Karl Storz 26003AA 10mm slender scope, are connected to a video processor. This processor can enhance image quality, manage white balance, and convert the sensor signal to a video signal to transmit the video to the operating room's screen. The analysis aims to determine the feasibility and efficiency of low-cost imaging systems in comparison to established technology in current use. Table 1 includes all sensors evaluated in the objective image tests and their supplied specifications. Vendor information for these sensors is available in Appendix 1.1.

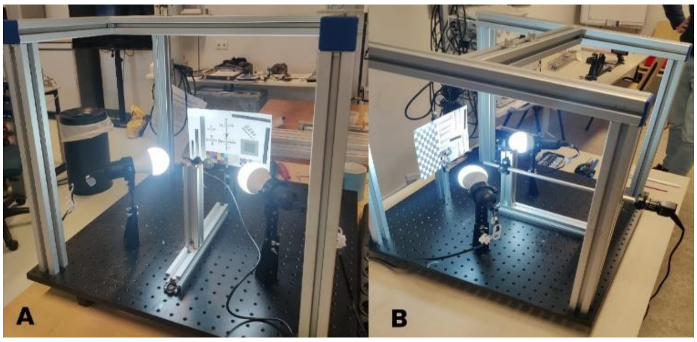

Figure 1: Test setup without cover at the MISIT lab (A) and the BovenIJ hospital (B).

A test setup was devised based on the requirements of the Imatest software to ensure identical conditions for each image captured for all imaging systems and to adhere to the standards of the performed tests[17]. This setup included a frame, depicted in Figure 1, which was covered with a thick, dark cloth or tarp to block external light sources. A test target was illuminated using two light sources positioned at 40-degree angles on either side of the target, as described in Imatest's test setup requirements, which aim to minimize glare [17]. These light sources emitted light at a color temperature of 6500K and an intensity of 2200 lux at the target. Image tests for the low-cost sensors were conducted at the TU Delft MISIT lab, while the commercial scopes were evaluated at Bovenij Hospital, as shown in Figure 1.

1.2.2: Image capturing and metric sourcing

Objective and subjective evaluations are essential to assess the performance of imaging systems for surgical use. For all low-cost imaging systems, the images are captured in Windows using the Amcap software. In contrast, commercial laparoscopes utilize proprietary capturing software. It is crucial to note that all images are recorded without any enhancement modes, which are available in some smartphone-based imaging systems and commercial laparoscopes.

The testing protocol, conducted in Imatest Master, the industry standard in automated image analysis, is categorized into six key areas: validation of suppliers' claims, sharpness, color, tone and noise, distortions, and imaging software.

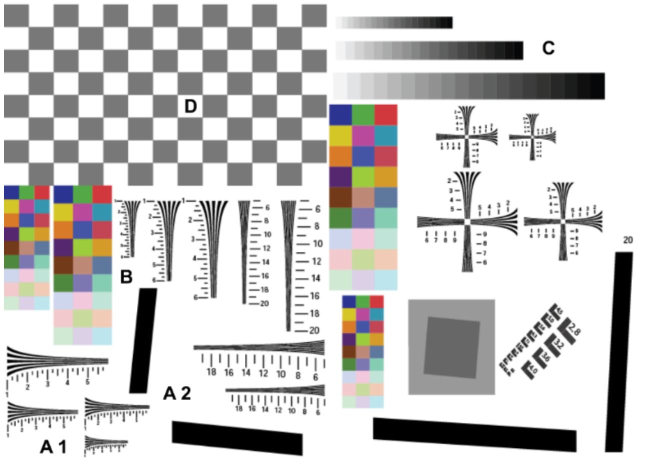

Figure 2: The used test charts where the sharpness components noted by A1 and A2, Color noted by B, tone and noise noted by C, and distortion noted by D are used.

The basis for the tests is the ISO 19264 standard for imaging[14], with additional topics and metrics based on Imatest documentation[17] and medical imaging standards such as ISO 8600 and ISO 12233 noted in papers and books[18, 19, 27].

Though no comparative values were accessible for endoscopic/laparoscopic devices, the result will be competitive between the imaging systems.

To ensure that the resolution of the test image does not constrain the measurements, the original vector files for the test images in Imatest were acquired from the creators of the charts, and the selected elements are combined into two charts, as shown shown in Figure 2. The charts were printed with a specialty high-quality and color-calibrated printer at 1200 dpi.

Table 1: Imaging systems specifications.

Sensor name:	**Stryker 1688 AIM 4k**	**Olympus OTV S7 Urology**	**Sony IMX 258 (IMX 258)**	**OmniVision 5693 (OV5693)**	**OmniVision 9734 (OV9734)**
Sensor size:	Not specified	Not specified	1/3.06 inch	1/4 inch	1/9 inch
Type of sensor:	Three chip CMOS	CMOS	CMOS	CMOS	CMOS
Resolution options:	3840x2160 - 1920x1080 Pixels	768x504 Pixels	3264 x 2448 - 1920 x 1080 pixels	2592 x 1944 - 1280 x 720 pixels	1280 x 720 - 640 x 480 pixels
Frame rates:	60 fps	60 fps	10 - 60 fps	15 - 60 fps	30 fps
Resolution tested:	1920x1080 pixels	768x504 Pixels	1600x1200 (FOV) 1920x1080 pixels	1600x1200(FOV) 1920x1080 pixels	1280x720 pixels
Field of view:	Depends on scope	Depends on scope	75 degrees	120 degrees	90 degrees
Cost:	25000 euro	10000 euros	42 euros	16 euros	90 euros
Focus:	Automatic	Variable	Automatic	Fixed	Fixed

1.2.3: Validation of suppliers' claims

The FOV is tested to validate the vendor's claims. The test is performed by capturing an image in the native aspect ratio of the sensor. A printed 16:9 and 4:3 rectangle, 192mm by 108mm and 160mm by 120mm, as shown in Figure 3, are used. The sensor is centered at the rectangle and then moved backward until the rectangle is at the image's border. Based on the tangential relation, the FOV can be determined in horizontal, vertical, and diagonal degrees, as in ISO 8600-3[18].

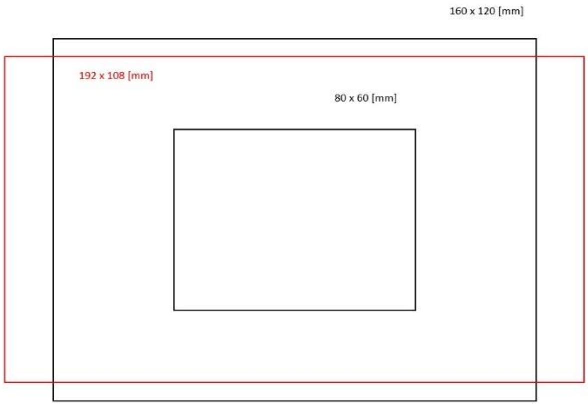

Figure 3: Test chart for determining the field of view of each imaging system.

1.2.4: Sharpness

Sharpness is seen as the most important factor for image quality[19]. This aspect is objectively measured using contrast's modulation transfer function (MTF) and the 10-90% rise distance at 100mm and 50mm working distances. The industry standard for imaging sharpness is the MTF50 value, which indicates the frequency of black and white cycles that fit per pixel while maintaining 50 percent of the initial contrast [20, 25]. This metric, expressed in cycles per pixel, facilitates comparison across systems with varying resolutions [25]. The 10-90% rise distance measures the number of pixels between 10 and 90 percent of the contrast.

Imaging systems with higher resolution, greater MTF, and a shorter rise distance between edges will be perceived as having sharper images [26].

The images produced by the assessed imaging systems are not raw and, therefore, are subject to processing and compression into specific formats by manufacturers. This process potentially allows for corrections or alterations to the image through software, a common practice that can impact the analysis. Most often, sharpening techniques, which enhance contrast around edges, are employed, thereby increasing the MTF50 frequency and the perceived quality of the image [19, 21].

This sharpening effect is quantified using the peak MTF value, where a value of 1 represents normal contrast, and values above 1 indicate the presence of sharpening [21].

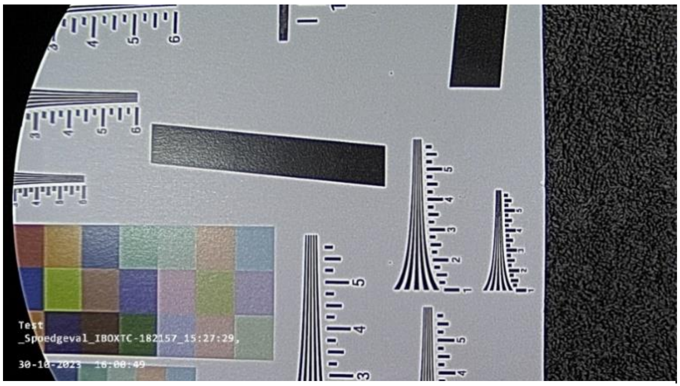

Figure 4: Maximum image enhancement setting on the Stryker 1688 showing hallowing artefacts.

Commercial laparoscopes are equipped with image enhancement modes that amplify these post-processing effects. However, these enhancements do not necessarily reflect the intrinsic quality of the imaging systems [21]. When these modes are fully activated, the contrast could be amplified up to three times the original, producing images with white halos around the edges, as illustrated in Figure 4. These sharpening algorithms typically show greater efficacy on straight lines and high-contrast edges. Therefore, both linear and nonlinear sharpness tests are conducted to assess sharpness. Based on slanted edges and wedges, these tests adhere to the guidelines set forth in ISO 12233 [19, 27]. The wedges and slanted edges used in the tests are noted with A1 and A2 in Figure 2.

Acutance, derived from the slanted edge, is utilized to compute perceived sharpness on a screen. This calculation integrates the MTF curve of the imaging system, the human eye transfer function, the range of viewing distances, and the size and type of the screen [28]. It allows for determining a sharpness score, ranging from 0 to 100, across various distances between the viewer and the screen. In the context of laparoscopy, surgeons typically view the monitor from a distance between 90-303cm, with the most common distance being around 150cm [22]. For low-cost laparoscopic systems, the display is often a 15-inch laptop screen. Considering these parameters, an acutance curve can be established, providing a subjective assessment of perceived image sharpness at different distances from the laptop screen.

1.2.5: Color

In the field of imaging, color accuracy, white balancing, and luminosity are quantitatively assessed using Delta E, Delta C, and Delta L metrics. These metrics represent the deviations in color and luminosity between the target and the captured image. Specifically, Delta E measures the overall deviation, while Delta C focuses on color space deviation, and Delta L quantifies the luminosity difference. These deviations are calculated based on differences in the 'a' and 'b' values, which represent a 2D color mapping, and the 'L' value, which denotes luminosity [14, 29]. The Universal Test Target (UTT) color test chart is employed for color analysis, as noted with a B in Figure 2 [14]. For comparability, the widely accepted Adobe RGB color space is utilized as the reference standard [29].

1.2.6: Tone and noise

The tone and noise characteristics of imaging systems are evaluated using the Kodak Q-13 chart, focusing on exposure error, gamma, contrast, and noise [14, 30]. Exposure error is quantified such that a value of 0 indicates ideal exposure. Negative values signify underexposure, resulting in a darker image than reality, while positive values indicate overexposure. Exposure is expressed in f-stops, which denote the lens's focal length ratio to the aperture diameter, which is inversely related to the amount of light captured on the image sensor.

The gamma value illustrates the relationship between pixel value and actual luminance. It represents the correlation between input and output signal brightness. A gamma value of ½ suggests linear brightness processing across all tones in the chart, while lower values indicate enhanced brightness in darker image areas to differentiate more tones [23].

The contrast ratio is determined by comparing the difference between the chart's white background and black lines. This metric is indicative of the discernible contrast levels between black and white [23].

Finally, pixel noise is assessed as the error in the tone color of the pixels. It is expressed in signal-to-noise ratio (SNR) and color difference percentage. An image is considered clear if the SNR is at least higher than one or 0 dB. This clarity is tested across a range of normalized exposures, from -35 at the darkest to 0 at the brightest tone, as noted with C in Figure 2 [31]

1.2.7: Distortions:

The chosen method for evaluating distortion in imaging systems involves the use of a checkerboard test chart noted with a D in Figure 2. This chart, intended to span the entirety of the captured image, allows for comparison between the actual straight lines on the physical chart and their representation in the captured image [14]. The assessment adheres to the SMIA TV distortion standard, which is a measure of the barrel, pincushion, perspective distortions, and chromatic aberrations into a single value. This value is expressed as a percentage deviation from the standard. The maximum barrel distortion is determined by examining the radius with the most pronounced horizontal and vertical distortions, providing an overall representation of the barrel distortion present in the image [32]

1.2.8: Displaying Software

Tests were conducted using the IMX 258 system at a distance of 100mm to discern differences in sharpness between different displaying software programs. During these tests, the system's autofocus was manually adjusted for both the wedge and the slanted edge. Images were screen captured in Windows for the various software programs, including Resolume Avenue, Touchdesigner, and Amcap. The MTF 20 and 50 were used as metrics to represent the sharpness over the MTF curve.

1.3: Results

1.3.1: Validation of suppliers' claims

As summarized in Table 2, the test findings indicated that all low-cost imaging systems aligned with their advertised FOVs. The OmniVision 5693 notably exceeded its expected FOV, while other low-cost systems marginally fell short. The Karl Storz lens, representing state-of-the-art technology, was measured at a diagonal FOV of 91 degrees. A lesser discrepancy between horizontal and vertical resolution was observed in the IMX 258 and OV 5693 imaging systems due to their 4:3 aspect ratio. In contrast, the OV9734 sensor, with a 16:9 aspect ratio, demonstrated a more significant difference between horizontal and vertical angles, affecting its diagonal FOV.

Table 2: Measured field of view (FOV) of all the imaging systems and their advertised FOV.

Sensor name:	**Stryker 1688**	**Olympus OTV S7**	**Sony IMX 258**	**OmniVision 5693**	**OmniVision 9734**
Advertised FOV	Wide view	Wide view	75° Diagonal	120° Diagonal	90° Diagonal
Measured FOV	75° Horizontal 52° Vertical 91° Diagonally	75° Horizontal 52° Vertical 91° Diagonally	56° Horizontal 43° Vertical 70° Diagonally	95° Horizontal 78° Vertical 122° Diagonal	72° Horizontal 44° Vertical 84° Diagonally

1.3.2: Sharpness

The sharpness test is divided into two segments for each distance. The sensor analyzes a wedge and a slanted edge target for each distance. The results yield MTF contrast over frequency curves for both distances and test types, with the slanted edge also generating an acutance curve based on factors such as the surgeon's position, monitor size, and type. Table 3 presents the MTF peak, MTF50 values, rise time, and acutance score, assuming a surgeon's viewing distance of 150cm from a 15-inch laptop monitor. Based on these metrics, it was found the Sony IMX 258 provides the sharpest images, followed by the Stryker 1688 and OV5693.

Table 3: Measured sharpness metrics for the Imaging systems.

Sensor name:	**Stryker 1688**	**Olympus OTV S7**	**Sony IMX 258**	**OmniVision 5693**	**OmniVision 9734**
MTF peak wedge-edge	1.18 – 1.44	1.00 - 1.03	1.03 - 1.11	1.01 - 1.02	1.00 - 1.01
MTF50 wedge (50 mm -100mm)	0.10 – 0.17	0.08 - 0.14	0.11 - 0.19	0.09 - 0.20	0.08- 0.10
MTF50 slanted edge (50mm - 100 mm)	0.09 - 0.24	0.10 - 0.10	0.19 - 0.31	0.11 - 0.19	0.10 - 0.13
10-90% Rise distance (slanted edge 50 - 100mm)	4.69 - 1.74	5.83 - 5.19	4.02 - 1.35	5.37 - 2.55	10.83 - 3.95
Acutance (50mm – 100mm) at 1.5m	74(C+) 121(A+)	44(F) 44(F)	93(A) 99(A+)	71(C+) 89(A)	39(F) 63(C)

MTF 50: For both test targets at both distances, it can be found that the IMX 258 reproduces the sharpest image, followed by the OV5693 and Stryker 1688. It is observed that the variance in the MTF50 scores for the OV5693 and OV9734 shows a similar trend regarding the difference in the wedge and slanted edge tests. However, when observing a linear slanted edge, the sharpness is significantly increased for the Stryker 1688 and the IMX 258. This suggests that the processing board employs an algorithm that sharpens the image even when enhancements are turned off, which is most effective for linear and clearly distinguishable lines.

While straight lines are most effectively enhanced, curved lines or complex textures are less affected by sharpening, as can be noted by the difference in peak MTF between the wedge and edge for the imaging systems, which exceed a peak MTF of 1.

Rise distance: The 10-90% rise distances measured conclude that the pixel distance for the IMX 258 and the Stryker systems are the shortest, which relates to a sharper image followed closely by the OV5693, with the OV9734 and the Olympus sensors trailing behind with a significantly larger distance. The effects of sharpening, which shortens the distance in pixels, are apparent here as well, resulting in shorter pixel distance values.

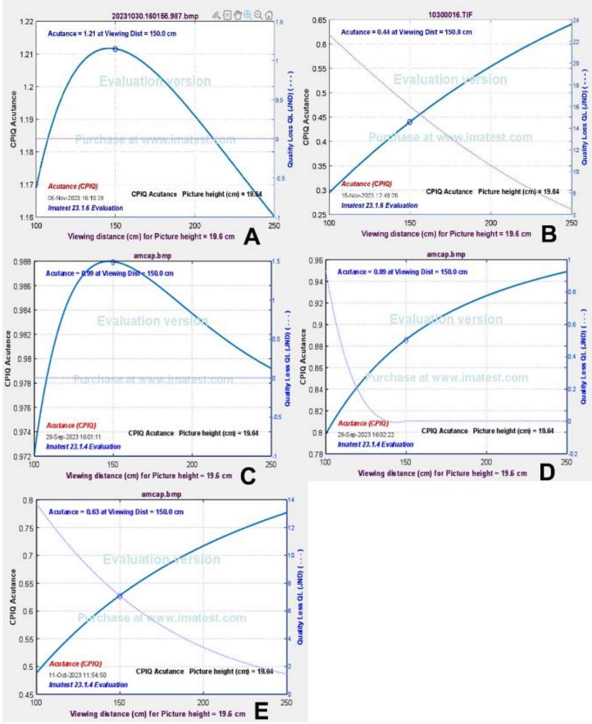

Figure 5: Acutance curves over distance to the screen for the Stryker (A), Olympus (B), IMX 258 (C), OV5693 (D) and OV9734 (E).

Acutance: The effect of sharpening also applies to the acutance since this is determined based on Imatest's slated edge MTF function. It is not yet included in tests such as wedges. In general, where there is no large amount of sharpening, the acutance function is expected to be monotonically increasing. The effect of increased contrast is expressed as an MTF peak in Table 3, which shows that the IMX and Stryker systems have inherent sharpening, and this shows in the not monotonically increasing acutance curve in Figure 5. However, the effect of sharpening when not exceeding a peak MTF of 1.30 could benefit the perceived sharpness without introducing artifacts to the image.

1.3.3: Color

The test assesses color reproduction, white balancing, and luminosity using Delta E, Delta C, and Delta L metrics, with mean and maximum values for each detailed in Table 4. This analysis provides insights into each system's performance in these areas. Based on these metrics, it was found the Sony IMX 258 reproduces the color the most accurately, followed by the OV5693 and Stryker 1688.

*Table 4: Measured *ab color metrics for the tested imaging systems.*

Sensor name:	Stryker 1688	Olympus OTV S7	Sony IMX 258	OmniVision 5693	OmniVision 9734
Delta E mean	31.6	37.6	16.9	23.1	36.7
Delta E max	54.3	71.3	43.6	53.8	69.7
Delta C mean	21.0	25.7	15.2	22.1	27.7
Delta C max	49.5	63.7	41.9	52.4	65.1
Delta L mean	11.2	19.7	5.3	6.3	18.8
Delta L max	25.2	28.2	14.1	26.5	29.9

Delta E: Regarding the overall color accuracy, the study uses the a, b, and L scales. The Sony IMX 258 exhibits the highest fidelity in color reproduction. Figure 6 visually demonstrates this accuracy, where the colors from the test chart (represented by large dots) closely align with their ideal positions (indicated by squares). This alignment reflects the deviation in luminance and color accuracy, calculated as Delta E. The IMX 258 performs the best in color reproduction, followed by the OV5693 and Stryker. The Olympus and OV9734 scored significantly worse on the mean and max errors.

Delta C: Regarding the white balancing, the IMX 258 maintains the balance with the lowest error, particularly in the red and green spectrums. In contrast, the Bayer color filter pattern in sensors like the OmniVision 5693 causes red color dominance or 'blooming,' especially under high light intensity, leading to color smearing. Based on Figure 6, it can be concluded that the OV5693 has a slight red hue found on the more saturated red pixels at the test luminosity. On the contrary, the Stryker and Olympus sensors seem to have a blue hue, which has to do with the saturation of these pixels, which seems to be a more elaborate choice.

Delta L: Luminosity, the key to vivid and distinct color tones, is best reproduced by the IMX 258 and OV5693, followed by the Stryker. The OV9734 and the Olympus sensor fall short, likely due to the light intensity.

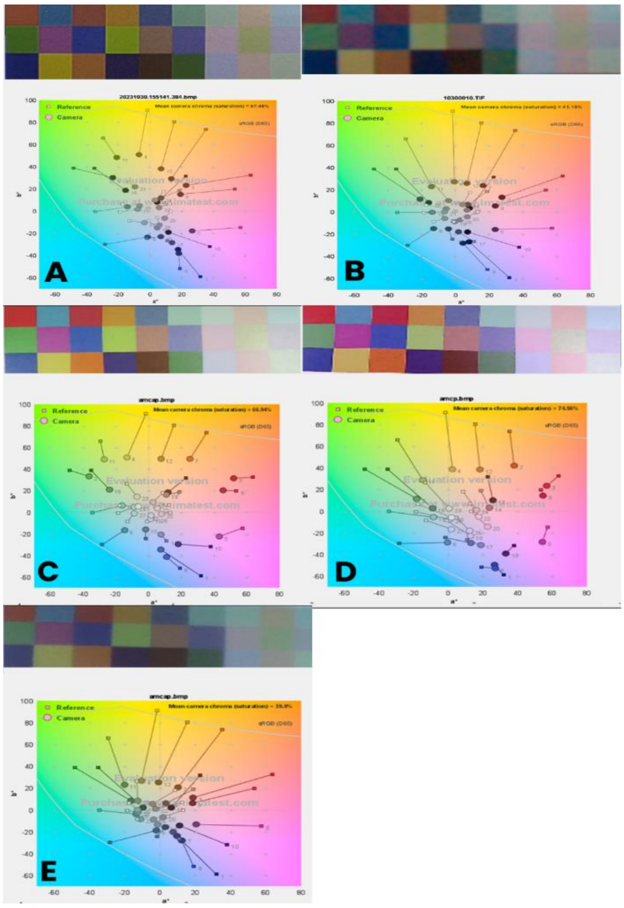

Figure 6: Color accuracy based on Adobe RGB color space for the Stryker (A), Olympus (B), IMX 258 (C), OV5693 (D), and OV9734 (E).

1.3.4: Tone and noise

The Kodak Q13 target test evaluates tone and noise using six chosen metrics: exposure error, gamma, contrast, pixel noise, and SNR. The results, detailed in Table 5, provide insights into tonal reproduction and the noise in the imaging system. Based on these metrics, it was found that the OV5693 is most effective at reproducing tone with minor noise.

Table 5: Measured Tone and Noise metrics for all imaging systems.

Sensor name:	Stryker 1688	Olympus OTV S7	Sony IMX 258	OmniVision 5693	OmniVision 9734
Exposure error	-0.94f-stops	-0.28f-stops	-1.37f-stops	-0.10f-stops	-1.65f-stops
Gamma	0.39	0.47	0.32	0.48	0.39
Contrast ratio	17.20	24.00	23.70	49.10	9.50
Pixel noise mean	1.10%	0.71%	0.65%	1.18%	0.48%
Exposure at SNR of higher than 1	-9.75f-stops	-1.22f-stops	-33.27f-stops	-35.00f-stops	-35.00f-stops
Peak SNR	19.75	21.00	32.25	27.50	28.50

Exposure Error and Gamma: The test reveals significant differences in exposure errors. The Sony IMX 258 and OmniVision 9734 have higher exposure errors (-1.37 and -1.65 f-stops, respectively), implying a need for more light to achieve saturation across all tones. In contrast, the OV5693 (-0.10 f-stops) and Olympus OTV S7 (-0.28 f-stops) exhibit lower errors, indicating better saturation. Gamma values, reflecting tonal balance, are more balanced in OmniVision 5693(0.48) and Olympus (0.46), compared to the IMX 258 (0.32), Stryker (0.39), and OmniVision 9734 (0.39).

Contrast ratio and Pixel Noise: The contrast ratio varies considerably, with OmniVision 9734 at the lower end (9.55) and OmniVision 5693 at the higher end (49.1), denoting their differing abilities in tone differentiation. Pixel noise mean is lowest in OmniVision 9734 (0.48%) and highest in OmniVision 5693 (1.18%), indicating varying efficiencies in color noise management.

Peak SNR: The Sony IMX 258 leads with a peak SNR of 32.25, suggesting high-quality image reproduction in terms of signal-to-noise. The peak SNRs for OmniVision 5693 (27.50) and 9734 (28.50) also indicate good quality, while Stryker 1688 (19.75) and Olympus OTV S7 (21.00) have slightly lower values.

Exposure at SNR > 1: This metric is crucial for understanding noise performance in low-light conditions. Olympus OTV S7 and Stryker 1688 show lower thresholds (-1.22 and -9.75 f-stops, respectively), indicating poorer performance in darker environments. Conversely, the Sony IMX 258, OmniVision 5693, and 9734, with thresholds at -33.27, -35.00, and -35.00 f-stops, perform better in low light, maintaining less noise in the image.

1.3.5: Distortions

The checkerboard test assesses image sensor distortions, with results presented in Table 6. This table includes overall SMIA TV distortion and the maximum distortion observed at the outer corners of the image. Based on these metrics, it was found the Sony IMX 258 has the least number of distortions in the image, followed by the Olympus OTV and Stryker 1688.

Table 6: Measured distortion metrics for the imaging systems

Sensor name:	**Stryker 1688**	**Olympus OTV S7**	**Sony IMX 258**	**OmniVision 5693**	**OmniVision 9734**
SMIA TV Distortion	-3.7%	-4.9%	-0.5%	-7.7%	-16.2%
Max barrel distortion	35%	20%	20%	60%	250%

SMIA TV Distortions: The level of SMIA TV distortion varies among the sensors. The Sony IMX 258 shows minimal distortion at -0.5%, indicating a close adherence to the SMIA TV standard with fewer distortions. The Olympus OTV S7 and Stryker 1688 demonstrate moderately higher distortion levels at -4.9% and -3.7%, respectively. The OV5693 registers a higher average distortion at -7.7%, and the OV9734 exhibits the most significant distortion at -16.2%

Max Barrel Distortion: The maximum barrel distortion observed differs across the sensors. The Olympus OTV S7 and Sony IMX 258 sensors display the lowest maximum barrel distortion at 20%. The Stryker 1688 has a slightly higher distortion at 35%, followed by the OV5693, with a maximum distortion of 60%. As anticipated, the OV9734, with its smaller sensor size and higher FOV, exhibits the highest barrel distortion at 250%.

1.3.6: Displaying Software

The sharpness test, conducted using three different software programs, indicates that the choice of software significantly influences image sharpness. Table 7 details the results, including cost, additional features, and resolution options.

Table 7 Comparison of Sharpness Metrics and Features Across Different Software

Software:	**Resolume avenue**	**Touchdesigner edu**	**AMCap**
MTF 20 - 50 wedge	0.48 - 0.35	0.29 - 0.21	0.40 - 0.29
MTF 20 - 50 edge	0.80 - 0.52	0.37 - 0.28	0.52 - 0.40
Price	75-299 euro	Free	Free
Resolution options	No restrictions	1280x720	1920x1080
Additional feature	Added sensor controls, sharpening, hue adjustment, color filter, zoom, gamma control and button mapping	Hue adjustment, color filtering, zoom and button mapping	none

MTF20-50 Results: The test demonstrates that Resolume Avenue produces a significantly sharper image, even without activating additional sharpening features, compared to Touchdesigner edu and AMCap. In the case of the IMX 258 sensor, the effect of inherent sharpening is evident across all software, but it is particularly pronounced with Resolume Avenue.

1.4: Discussion

The primary goal of this study was to identify the most suitable sensor for low-cost laparoscopes by comparing it to current imaging systems used in Western hospitals. The tests revealed that the differences between the sensors were subtler than expected, though certain factors may have influenced the results.

1.4.1: Test setup and imaging capturing limitations

In the testing conducted at Bovenij Hospital using the Stryker 1688, the sensor's full-resolution capabilities were not used. The sensor was configured to Full HD instead of its native resolution, primarily because the hospital's monitors did not support 4K resolution.

Additionally, a significant difference was noted between the brightness levels on the screen and those in the captured images. This issue became apparent after analyzing the recorded images received a few days post-measurement.

For the comparative analysis, a 7mm endoscope sensor was initially procured. However, during preliminary testing, this sensor ceased transmitting an image signal, which coincided with excessive heat emission.

Due to unexpected damage to the Kodak Q13 chart before testing the OV9734 sensor, which was only available for a few hours, a new semi-reflective chart was used instead of the preferred reflective chart. This new chart was consistently used for all subsequent measurements to ensure comparability across imaging systems.

The cover over the test setup effectively blocked external light, but the color was not optimal for the Color and Tone and Noise measurement. Ideally, an 18 percent gray surrounding is advised by Imatest for the most accurate tone and noise measurements.

The imaging systems tested utilize various methods to focus light onto the image sensor, and these differing approaches can significantly impact the sharpness of the resulting images. During the sharpness tests, it was observed that the autofocusing of the Sony IMX 258 imaging system struggled with consistent focusing at close ranges, specifically between 40mm and 100mm. The sharpness test only used correctly focused images, though this could be a problem for the use as an imaging system for a laparoscope.

1.4.2: Field of view Measurements

The aspect ratio of image sensors, particularly in mobile phone sensors, predominantly follows a 4:3 ratio, while screens for video playback often use a 16:9 ratio.

This disparity necessitates scaling images from a 4:3 resolution, such as 1600x1200 pixels, to fit a 1920x1080 screen, which can lead to changes in sharpness and the potential creation of artifacts. For sensors like the IMX 258 and OV5693, using a 16:9 ratio results in a reduced diagonal FOV of 65 degrees and 110 degrees, respectively, impacting the overall image quality.

In the case of commercial laparoscopes, the FOV was not explicitly measured for both devices. It was assumed that the lens would be the limiting factor for FOV; therefore, only the Stryker laparoscope was measured. However, subsequent assessments indicated significant differences, such as the maximum distortion. The Stryker laparoscope displayed a larger FOV, while the Olympus laparoscope could not fully utilize the FOV offered by the Karl Storz lens. As a result, the FOV of the Olympus laparoscope system is likely lower than what is stated in Table 2.

1.4.3: Sharpness Measurement

An increase in image resolution, characterized by a higher pixel count covering the same area, can significantly enhance the detail and contrast at the edges of an image. This enhancement typically results in a higher MTF50 value and, consequently, a higher acutance score. The finer spatial resolution offered by higher-resolution images also improves the effectiveness of edge-sharpening techniques, contributing to an overall increase in the perceived sharpness of the image. Therefore, the Stryker imaging system, when using its native resolution, should have significantly better results than what is noted in Table 3.

The rise distance metric presents a challenge when comparing image sensors with varying resolutions. Different resolutions mean that the same edge in a scene is represented by a varying number of pixels across different images. A sensor with a higher resolution may display a more gradual transition (a larger rise distance) due to its more significant number of pixels that distribute the transition over a wider area. Therefore, it is only more pronounced that the three full HD sensors have shorter transitions while having 2-4 times more pixels than the Olympus and OV9734 imaging systems.

Commercial laparoscopes often include image enhancement functions designed to increase image quality for a surgeon. It was observed that these enhancements could amplify the sharpening effect several-fold. However, it's important to note that a peak MTF value higher than 1.30 can introduce artifacts into the image, potentially degrading image quality.

Despite this, the capability of high levels of sharpening in commercial laparoscopes suggests that, under certain conditions, increased sharpening may enhance the image quality for laparoscopic applications.

1.4.3: Color Measurement

The discrepancy observed in the brightness levels between Stryker's measurements and the recorded images might have contributed to the substantial mean luminance delta noted. Suppose the luminance setting during the measurements had been higher than the utilized level of 3 out of 7. It could be that the difference and, therefore, resultant error in luminance delta could have been lower.

An experienced laparoscopic surgeon involved in the project highlighted two critical factors that can significantly affect image quality, often not accounted for in the testing of laparoscopes. The first is blood flow during surgery, which can induce blooming. This blooming effect can obscure fine tissue details, making differentiation challenging. The second factor is the introduction of smoke in the surgical area, which can pose processing challenges for some imagining systems.

1.4.4: Tone and Noise Measurement

The exposure at which the SNR exceeds 1 is measured in f-stops to determine the minimum light quantity needed for a discernible image. While this metric is not standardized for tonal reproduction, it provides valuable insights into image noise. Notably, the contrast between low-cost imaging systems and commercial laparoscopes is most apparent in tone and noise assessments. The higher noise and exposure errors in commercial systems might be due to their testing under light intensities significantly lower than the 5-10 times higher intensities typically used in conventional laparoscopic surgery.

The measurements are based on one image of the same chart; therefore, a random aspect, such as the noise, might differ for each image taken. The general Noise results could, for this reason, fluctuate. Capturing multiple images and averaging the results could result in a more accurate measurement of the noise of the imaging systems. It is deemed that the rest of the tested image quality factors were not influenced based on this fact.

1.4.5: Distortion Measurement

The distortion levels depend on the sensors and lenses' physical and geometrical properties and post-processing. Since these systems directly provide an image, the actual effects of the processing could go unnoticed. Commercial laparoscopes use different slender scopes, making image correction impossible. The imaging system, which combines lenses and sensors, could employ such methods, although this was not observed during testing.

1.4.6: Influence of Software on the Image Quality

Using screen captures to record images adds an extra variable as the processed and displayed image undergoes further processing and saving.

Screen captures may lead to compression and alterations in image quality, potentially amplifying differences between software. Besides, the AMCap software's inability to create a full-screen image might compress the image, introduce artifacts, and diminish sharpness. While sharpness is a crucial image quality factor, other aspects like vividness and noise also play significant roles. Though not measured, a noticeable difference can be observed visually.

1.5: Conclusion

This study focused on identifying an appropriate low-cost imaging system for a low-cost laparoscope by comparing these imaging systems with commercial laparoscopes. The evaluation prioritized FOV, image quality, and price to adhere to the low-income regions.

The measurement results indicated that the OmniVision 5693 imaging system is the most promising candidate. Its FOV, tone, and noise metrics exceed those of commercial laparoscopes. The OmniVision 5693 excelled in tone and noise reproduction, approaching saturation under a 2200lux light source, suggesting effective low-light performance. Its affordability also positions it as a suitable option for resource-limited settings.

While the Sony IMX258 offered sharper images and more accurate color reproduction, its inconsistency in focusing at close range made the OmniVision 5693 the more viable.

However, the study faced limitations. Variations in resolution and aspect ratios between sensors could have influenced the accuracy of the comparative analysis. External factors such as blood or smoke during surgery, which affect sensor performance, were not covered but are crucial in real-world applications. These factors require further investigation.

The impact of image-displaying software on the performance of low-cost imaging systems was also notable. The choice of software significantly affects the image quality as perceived by the surgeon, indicating a need for additional research into developing image-displaying software with similar image quality and essential features to reduce the cost.

In summary, the OmniVision 5693 imaging system is identified as a promising candidate for an affordable laparoscope, offering a balance between a large FOV, image quality, and cost-effectiveness. However, further research is necessary to address this study's limitations and untested variables, especially concerning real-world surgical conditions and software optimization. These findings will contribute to the second part of this thesis titled: 'Design and Development of a Modular 500-dollar Laparoscope using a Low-Cost Imaging System', which aims to improve laparoscopic access in low-income countries and rural settings with a sub 500-dollar laparoscope.

1.7: References

[1] G. Ahmad, D. Gent, D. Henderson, "Laparoscopic entry techniques," *Cochrane Database of Systematic Reviews,* 2015.

[2] A. Buia, F. Stockhausen, E. Hanisch, "Laparoscopic surgery: A qualified systematic review," *World Journal of Methodology,* vol. 5, nr. 4, p. 238, 2015.

[3] D. Duppler, "Laparoscopic instrumentation, videoimaging, and equipment disinfection and sterilization," *Surgical Clinics of North America,* vol. 75, nr. 5, pp. 1021-1032, 1992.

[4] M. Gaab, "Instrumentation: endoscopes and equipment.," *World neurosurgery,* vol. 79, nr. 2, pp. 11-21, 2013.

[5] M. Mohsin, T. Majid, I. Saleem, "Laparoscopic cholecystectomy in a small rural hospital in Kashmir Valley, India," *Tropical Doctor,* vol. 38, nr. 4, pp. 213-6, 2008.

[6] Y. Teerawattananon, M. Mugford, "Is it worth offering a routine laparoscopic cholecystectomy in developing countries?Is it worth offering a routine laparoscopic cholecystectomy in developing countries? A Thailand case study," *Cost effectiveness and resource allocation ,* vol. 3, p. 10, 10 2005.

[7] J. L. Mueller, N. Rozman, E. D. Sunassee, A. Gupta, C. Schuval, A. Biswas, B. Knight, S. Kulkarni, M. Brown, N. Ramanujam en T. N. Fitzgerald, "An Accessible Laparoscope for Surgery in Low- and Middle- Income Countries," *Annals of Biomedical Engineering,* vol. 49, nr. 7, pp. 1657-1669, 7 2021.

[8] S. Jawale, G. Jesudian, „Low-cost laparoscopy for rural areas: the flexible video laparoscope," *Tropical Doctor,* vol. 49, nr. 1, pp. 68-70, 1 2019.

[9] F. Gheza, F. O. Oginni, S. Crivellaro, M. A. Masrur, A. O. Adisa, "Affordable Laparoscopic Camera System (ALCS) Designed for Low- and Middle-Income Countries: A Feasibility Study," *World Journal of Surgery,* vol. 42, nr. 11, pp. 3501-3507, 11 2018.

[10] I. Chatzipapas, N. Kathopoulis, A. Protopapas, D. Loutradis, "Using a Mobile Smartphone to Perform Laparoscopy," *Journal of Minimally Invasive Gynecology,* vol. 25, nr. 5, pp. 912-915, 7 2018.

[11] Y. Takemura, "The Development of Video-Camera Technologies: Many Innovations Behind Video Cameras Are Used for Digital Cameras and Smartphone," *IEEE Consumer Electronics ,* vol. 8, nr. 4, pp. 10-16, 2019.

[12] T. N Trivedi, "An economical model for mastering the art of intubation with different video laryngoscopes," *Indian J Anaesth,* vol. 58, nr. 4, pp. 394-6, 2014.

[13] D. Zezo, "Laparoscopic/Robotic Camera and Lens Systems," Abdominal key, 2018.

[14] M. Nishibori, "Problems and Solutions in Medical Color Imaging," *Proceedings of Second International Symposium on Multispectral Imaging and High Accurate Color Reprocuction,* pp. 9-17, 2000.

[15] D. Wueller, "Standardization of Image Quality Analysis – ISO 19264," Image Engineering, Cologne, Germany, 2012.

[16] N. Fotiadis, M. Miah, E. Abel, "Defining optical distortion in rigid endoscopes," *The Laryngoscope,* vol. 125, nr. 3, pp. 561-566, 2014.

[17] N. Koren, "Targets," in *Imatest Documentation*, Imatest, 2019, p. 72.

[18] A. Khanicheh, D. Leiner, Q. WANG, "Endoscope field of view measurement," *Biomedical Optics EXPRESS,* vol. 8, nr. 3, pp. 1441-1453, 2017.

[19] M. Kaur, S. Kaur, "Image Sharpening Using Basic Enhancement Techniques," *International Journal of Research in Engineering, Science and Management,* vol. 1, nr. 12, pp. 122-127, 2018.

[20] H. H. Nasse, "How to Read MTF Curves," Carl Zeiss, 2008.

[21] N. Koren, "Comparing sharpness in cameras with different pixel count," Imatest, 2023.

[22] A. C. G El Shallaly, "Optimum view distance for laparoscopic surgery," *Surgical Endoscopy And Other Interventional Techniques ,* vol. 20, pp. 1879-1882, 2006.

[23] N. Koren, "Gamma, Tonal Response Curve, and related concepts," Imatest, 2023.

[24] R. Mishra, Textbook of Practical Laparoscopic surgery, New Delhi: Jaypee brothers medical publisher LTD., 2013.

[25] N. Koren, "Sharpness: What is it and How it is Measured," in *Imatest Doucmentation*, 2019.

[26] N. Koren, "MTF curves and Image appearance," in *Imatest Documentation*, 2019.

[27] N. Koren, "Sharpness comparisons for several digital cameras," in *Imatest Documentation*, 2019.

[28] N. Koren, "Acutance and SQF (Subjective Quality Factor)," in *Imatest Documentation*, 2019.

[29] N. Koren, "Color/Tone Interactive Analysis," in *Imatest Documentation*, 2019.

[30] N. Koren, "Using Stepcharts," in *Imatest Documentation*, 2019.

[31] N. Koren, "Tone, color and spatial modules," in *Imatest Documentation*, 2019.

[32] N. Koren, "Distortion: methods and modules," in *Imatest Documentation*, 2019.

Part 2: FlexMod Laparoscope: The design and validation of a low-cost laparoscope

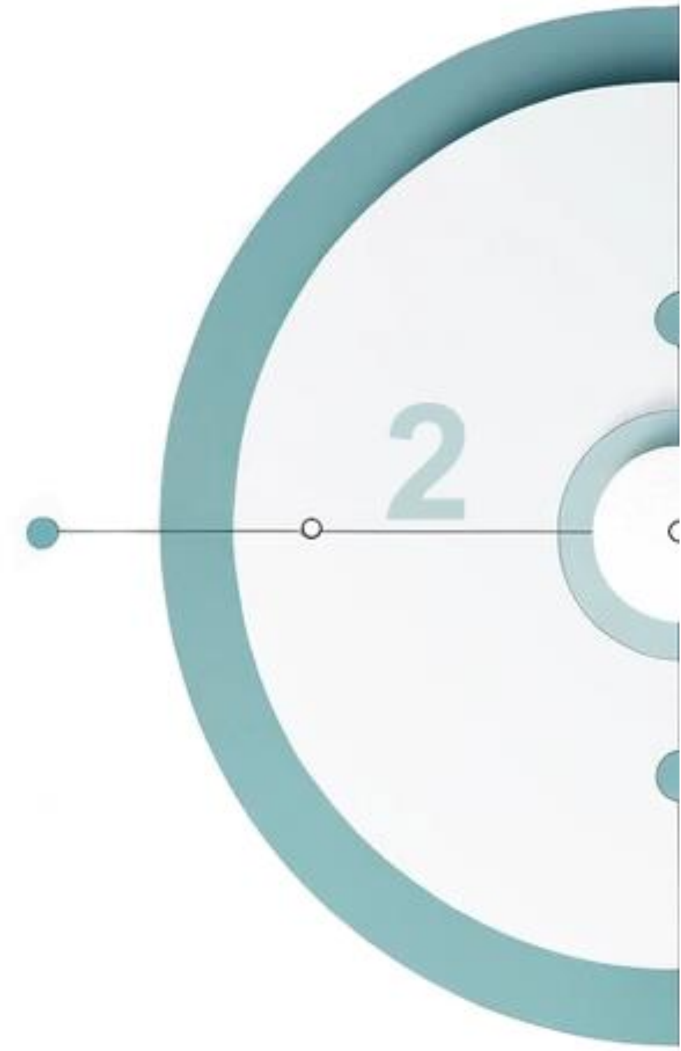

Autor: Rafael van Loon

Thesis committee: Prof. Dr. J. Dankelman, TU Delft, Chair

Dr. Ir. T. Horeman, TU delft

Design and evaluation of a modular sub-500-dollar laparoscope using a Low-Cost Imaging System

***Abstract*- The availability of laparoscopy in low-income settings has been limited based on the requirements that have to be met to perform this type of abdominal surgery. At the same time, these regions and countries could stand to gain the most from it based on quicker recovery times and a lower chance of infections. Attempts have been made to solve this inaccessibility by minimizing the required components to perform this type of surgery at a substantially lower cost. None of these projects have resulted in a laparoscope that can compete with commercial laparoscopes regarding resolution, image quality, and critical design features such as viewing angle. Based on these shortcomings, this study aims to design a sub-500-dollar modular laparoscope for gas and gasless laparoscopy that adheres to state-of-the-art image quality and design features. The laparoscopes are designed following the 'Roadmap for Design of Surgical Equipment for Safe Surgery Worldwide". Based on the roadmap requirements regarding the needs of patients, end-users, and stakeholders, were acquired focusing on cost, robustness, and reusability. Following the design process, two intermediate prototypes were developed, which were evaluated based on function and image quality by a laparoscopic surgeon to validate the requirements and receive design feedback. They resulted in a modular laparoscope that connects with USB to a laptop, which shares the image sensor, light source, electronics, and handle between the laparoscope for gas and gasless laparoscopy. The gasless laparoscope employs a flexible chip-on-the-tip design that can be straightened for entry through a trocar and released to set the tip angle at 30 degrees. The gasless laparoscope does not have to comply with the trocar and can enter straight through the abdominal entry point. Resulting in a chip-on-the-tip design, which is statically bent at an angle of 30 degrees. To validate the design, a laparoscopic surgeon evaluated the function and image quality, and additional tests were performed to validate the thermal and reprocessing capability. The study resulted in a modular sub-500-dollar laparoscope for gas and gasless laparoscopy, which shows great potential but requires future work to be certified and production-ready.**

2.1: Introduction:

2.1.1: Background of laparoscopy and its challenges

Medicine and healthcare aim to heal with minimal complications, ensuring patients' quick return to good health [1]. A current approach in modern medicine is the use of smaller incisions to perform conventional procedures. This field is fittingly called Minimal invasive surgery, where small incisions are created, and instruments are inserted inside the body instead of opening the body to inspect or operate on tissue [2, 3]. This method of reducing surgery's invasiveness and promoting faster recovery, better cosmetic results, and reduced pain for the patient is often used in abdominal surgery, which is called laparoscopy [2, 4, 5]. Standard procedures, such as the removal of the appendix, tubular sterilization, and gall bladder removal (cholecystectomy), are nearly exclusively performed laparoscopically, at least in the Western world [3, 6].

Geographical disparities in surgical approaches, notably in laparoscopy, are primarily driven by the costs of equipment and infrastructure required [7, 8, 9]. In many areas, particularly where resources are limited, the high expense of laparoscopic tools, training, and facilities often leads to reliance on more traditional laparotomy involving larger incisions [10]. However, these regions could benefit the most regarding the advantages since sick leave, reliable blood banks, and sanitary living conditions are not always expected, especially in more rural settings [11]. Laparoscopy is also emerging as a cost-effective diagnostic tool in LMICs compared to more expensive methods like ultrasound, CT, and MRI, with a cost ratio of 1:500:2500:4500 [12]. This lower initial cost is likely why 1/3 of laparoscopic surgeries in some African regions are diagnostic, although access remains limited for many [13].

2.1.2: Laparoscopic techniques and equipment

In order to perform laparoscopic surgery, an operating space in the abdominal cavity needs to be created to inspect and manipulate the tissue [2, 14]. The Lifting of the abdominal wall is often done by inserting a tube-like instrument through the abdominal wall that pumps carbon dioxide gas in, which internally inflates the abdominal cavity [2, 4, 14]. Special tube-like tools, trocars are used as a passageway for instruments to enter the abdominal cavity and prevent the gas from escaping [2, 4, 14].

Next is a laparoscope, as shown in Figure 1(B), which commonly consists of a camera head and a slender scope, often called a laparoscope itself. It is connected to a light source and inserted through one of the trocars, giving the surgeon a view of the abdominal cavity. At the same time, other trocars can provide passage to other instruments used to perform surgery within the abdomen, such as grippers and cutters.

The light source, the processing of the image through the scope, the regulation of the body's gas pressure, and the image's display are combined in one large and heavy installation, often called a laparoscopic tower [15], as shown in Figure 1(A) on the right. The initial purchasing cost of this tower can exceed 100,000-dollars [15] and requires large amounts of energy to operate, which is expensive and not always feasible for Lower and middle-income countries(LMICs) [8, 9]. Among these components, the illumination and imaging systems constitute the bulk of the cost, and they happen to be the most delicate and susceptible to damage when subjected to impacts or bending [17,18].

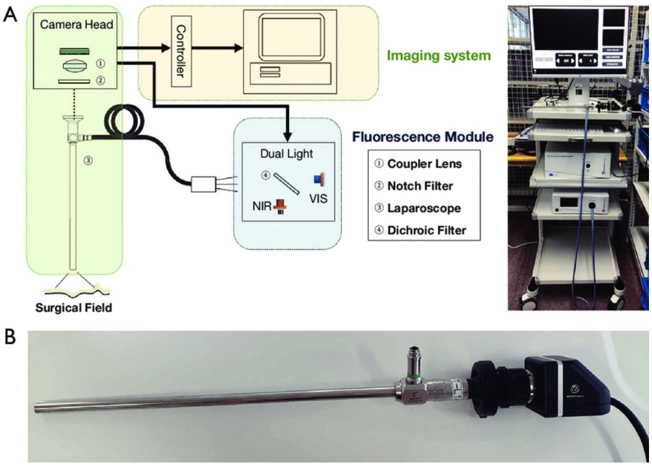

Figure 1: Laparoscopic tower set up (A) connected to the camera head and slender scope (B)[30]

2.1.3 Alternative methods and innovations

Alternative methods of performing laparoscopic surgery without gas insufflation have been proposed to reduce the need for the trocars, which can keep a seal and eliminate the need for the gas and the insufflator [19]. Instead, a physical device is used, which lifts the abdominal wall from the inside, as shown in Figure 2. This kind of laparoscopic surgery is often called gasless- or lift-laparoscopy [19, 20]. It also has other advantages not related to the price. Still, regarding the perceived pain in standard laparoscopic surgery, the whole body is sedated since the pressure exerted by the gas on the internal organs can lead to sensations of pain up to the shoulder. In contrast, gasless surgery could use local anesthesia [19, 20].

Projects in academia and start-ups have aimed to reduce the cost, reliance on constant energy, and robustness of laparoscopic instruments. The projects aim to reduce the highest cost of the laparoscope, video processor, light source, and display equipment. The solutions vary from attaching a smartphone to a slender scope [21] to using cheap, low-resolution borescope cameras primarily used for inspecting pipes for cracks connected to a laptop [22].

These academic projects try to eliminate as much of the laparoscopic tower as possible to reduce the price and increase the robustness and transportability for low-income countries and rural settings. The smartphone on a scope tries to integrate the camera head of the laparoscope, video processing and displaying in one part[21]. The solutions that integrate boroscope cameras often go a step further, including a light source and, when connected to a laptop, covering all the equipment needed to see inside the abdomen[22].

Figure 2: Abdominal wall physically lifted with a lift device with a laparoscope inserted into the abdomen [19]

2.1.4: Limitations of existing low-cost solutions

While these low-cost solutions are usable for some laparoscopic procedures, they exhibit significant deviations from state-of-the-art equipment, limiting their direct replacement potential. For instance, the smartphone design faces challenges such as a small screen that cannot be sterilized, necessitating drapes. Additionally, it relies on a fragile, slender scope lens that requires an external light source connected via optical fiber cables.

On the other hand, the borescope devices address some of these issues by relocating the sensor to the distal tip of the device, reducing the reliance on the slender scope with lenses, and enabling submersion in sterilizing agents when fully sealed in a shaft. However, it encounters problems with the sensor and processors connected to a single PCB. This configuration presents a three-fold issue: the borescope sensor's video resolutions are low, with low resolution being a common complaint from laparoscopic surgeons [17]. Besides, all the components are concentrated at the tip, which can generate significant heat during operation, and the lens is oriented straight forward. This straight orientation limits the scope's usability to minimal procedures, while the standard in most procedures calls for a 30-degree offset from the tip. This offset allows for comprehensive tissue inspection and enhances the observable field.

2.1.5: Design of a laparoscope

Based on the discoveries from the first part of this thesis, titled "Comparative Analysis of Low-Cost Imaging Systems versus Commercial Laparoscopes," a high-performing imaging system has been identified as a worthy contender against state-of-the-art laparoscopes regarding image quality and field of view (FOV).

The study revealed that an imaging system based on the OmniVsion 5693 sensor could deliver a full HD at 30 fps or HD ready at 60 fps video via USB without specific drivers or software. During the evaluation, it was recommended to use Resolume Avenue software until custom software could be developed to integrate external peripherals to control settings. Furthermore, the sensor was found to approach full saturation when exposed to a light source of 2200lux. This illumination level is required over the operating distances of the laparoscope to maximize the sensor's performance.

Goal: This study aims to integrate the image sensors selected in the first part of this thesis, integrating it based on the “Roadmap for Design of Surgical Equipment for Safe Surgery Worldwide”, in a low-cost laparoscope that can be used for gas and gasless laparoscopy in low-income countries and rural settings. The laparoscope will have an angled view of 30 degrees and integrate most to all parts required for imaging of the laparoscopic tower when connected to a laptop. It will go by the name of the FlexMod laparoscope and cost less than 500 dollars.

2.2: Method

2.2.1 Roadmap of Design of Surgical Equipment

For the design of the laparoscope, the needs and requirements are formed based on analyzing the needs of users and organizations. The roadmap proposed in 'Roadmap for Design of Surgical Equipment for Safe Surgery Worldwide' is followed to assess LMICs with a specific focus on sub-Saharan Africa and India context, based on the surgeons' needs and noted problems in the literature to perform laparoscopic surgery [24]. The requirements are obtained based on the barriers, healthcare system, and required aspects for safe laparoscopic surgery. Based on the analysis and required functions, functional and performance requirements are set for a context-driven design method.

This apparent need for specific surgical equipment is identified based on surgeons' input in the field and conditions expressed in the literature [12, 13, 21, 22, 24].

Regarding the gas and gasless laparoscopic fields, a renowned laparoscopic surgeon gave direct feedback based on his experiences in established modern hospitals and field hospitals in rural areas.

The surgeon is involved in gasless laparoscopy, noting its ability to eliminate the need for gas insufflation as a cost-effective and mobile solution, particularly in rural settings. The surgeon noted that for gas laparoscopy, the laparoscope should be able to fit through a commercially available trocar, and adherence to a 10 mm trocar is not strictly necessary since other sizes, such as 12mm trocars, are standard in most places. Moreover, laparoscopes intended for rural settings must exhibit enhanced durability due to different transport and storage conditions, minimizing vulnerability to damage when dropped, given the limited replacement part availability in these settings [16, 17, 18].

The main barrier encountered in adopting laparoscopy is the cost. These costs are divided into the initial cost of purchasing the laparoscopes and consumables [17]. Additional problems relating to the general adaptation and wider spread use of laparoscopy are related to the infrastructure, which is not always available [8]. An operating theatre must be relatively modern to facilitate the required laparoscopic tower to perform laparoscopy effectively. In regions in India and sub-Saharan Africa, a constant electricity source is not a given in all hospitals[22], making using (high power) electrical equipment that relies directly on the electrical grid less reliable. This includes devices disinfecting the instruments, which often use large amounts of energy, such as a steam autoclave.

The complexity of laparoscopes necessitates repair and maintenance services that may not be readily accessible in all regions [17]. The difficulties of reprocessing and required training for proper instrument use and reuse add to the challenges [29]. Besides demanding specialized training, laparoscopy often requires more time to perform than equivalent laparotomic procedures[29].

Since the procedure requires more expensive instruments and specific training, it is not always employed in all hospitals. Hospitals in India and sub-Saharan Africa are generally part of private or public healthcare systems. Where public hospitals are primarily state-funded and cater to the economically less fortunate section of the population, these hospitals cover most to all of the costs of the procedures. The private system is extensive and diverse, catering to the population that can pay the cost out of pocket or through private health insurance. These hospitals have state-of-the-art infrastructure, equipment, and laparoscopic surgeons.

2.2.2 Requirements and Concept Evaluation

Based on the findings of the roadmap analysis, this section continues the process by outlining the methodology used in the context-driven design of a modular laparoscope, integrating the context-related analysis with functional operational requirements. The design process employs a convergent approach, combining a morphological assessment and a Harris profile evaluation to select the most promising design to develop into a final design.

The noted functional requirements serve as essential criteria that any conceptual design must fulfill.

● Cost Efficiency: *The laparoscope's initial purchasing price does not exceed $500, ensuring affordability.*
● No Consumables: *The design should eliminate the need for consumables, like drapes.*
● Imaging System: *Incorporation of the OmniVision 5693-based imaging system is mandatory.*
● Shaft length: *In order to reach the tissue in the abdomen, the distance from the tip to the handle should minimally be 300 millimeters(mm).*
● Entering: *The laparoscope should be able to fit through a commercially available trocar to be used for gas laparoscopy.*
● Illumination: *The laparoscope should provide illumination exceeding 2200 lux at operating distance.*
● Weight Specification: *The device's mass should not surpass 1-2 kg, aligning with the state-of-the-art.*
● Disinfection Compatibility: *Materials must be compatible with High-Level Disinfection(HLD) solutions such as Cidex OPA and Glutaraldehyde.*
● Lens Orientation: *The lens should have a 30-degree offset from the slender rod for optimal functionality.*
● Temperature Regulation: T*he device temperature should not exceed 48 degrees Celsius during constant contact to prevent burns.*

The performance criteria, alongside end-user feedback, are pivotal in rating design concepts and converging towards a final design.

● Cost Impact: The cost is a significant factor in the adoption of laparoscopes, particularly in regions like sub-Saharan Africa. A lower-priced device can facilitate broader acceptance.
● Invasiveness: The scope's invasiveness relates to the diameter of its distal end, affecting the incision size and operative space for gasless laparoscopic surgery.
● Robustness: A robust design should minimize the use of fragile components like glass lenses and fiber optics, known for their frequent breakage in laparoscopes.
● Reprocessing Ease: Instruments should be designed for simple cleaning and sterilization, preferably as a single part, to avoid issues in disassembly and ensure effective cleaning and disinfection, particularly in low-income countries and rural settings.
● Repairability: The device should be repairable with locally accessible tools and spare parts to minimize downtime due to instrument failure.
● Versatility in Surgery: The scope's design should be suitable for most laparoscopic procedures. Its compatibility with standard trocar sizes (5, 10, 12, and occasionally 15mm) is crucial for this versatility.

Each criterion is weighted based on their perceived importance and rated on the specific metric, as noted in Table 1

Table 1: Performance requirements and their respective Harris profile weights

Criteria points	Specifics	Weight (points)
Cost	1: Component cost is lower than 100 euros. 5: Component cost of 300 euros.	10p
Invasiveness	1: Shaft diameter between 14-15mm 5: Shaft radius < 10 mm	10p
Robustness	1: Internal components made of brittle materials 5: Minimal use of brittle materials	10p
Ease of reprocessing ability	1: Disassemble and replace parts. 5: No disassembly and extra reprocessing steps required	7p
Serviceability	1: Not serviceable 5: Modular components	4p
Compatibility	1: Requires scope-specific instruments and software to operate. 5: Can use the equipment already in use	4p

2.2.3: Validation Methods

In order to validate that the functional requirements are met and to receive feedback from an end-user on the performance of the device, a set of four tests needs to be completed.

Illumination: The amount of light produced by the light sources in the scope will be assessed utilizing a lux meter, which determines the intensity of the light over the area of the measuring device. The light source will be placed at a set of distances (50, 100mm) that correlate to the working distances of a laparoscope to the tissue [28]. The aim is to measure values exceeding 2200lux at both distances from the target.

Thermal: The device comes in contact with the patient and surgeon and should, therefore, not exceed a temperature of 48 degrees at constant contact with users or patients. The temperature should not exceed 56 degrees for parts that come in touch for up to 60 seconds, which is seen as short contact.
Therefore, the shaft and the handle should not exceed 48 degrees, and the tip should not exceed 56 degrees. These temperatures are based on IEC 60601-1 [26].

The tip, shaft, and handle will be measured by an infrared temperature measuring gun, recording the temperature every 5 minutes for 180 minutes, emulating the duration of laparoscopic surgery [25] in a box-trainer to reduce the effects of convection cooling the tip and shaft down.

Reprocessing: The materials chosen for the external components will withstand exposure to the noted disinfectants as noted in[27], so the test will conclude if the device does not leak while submerging for one hour in a tank to reprocess the instrument at High-level disinfection specifications [18, 27]. The scope will be submerged to check if any air bubbles appear on the tank's surface.

User test: A laparoscopic surgeon will perform a maneuverability test in a box-trainer. The box-trainer is filled with a curved carton plate simulating different levels of height found in the abdomen, which is covered by an image capturing the colors found in the abdominal region. The surgeon should be able to put the laparoscope inside the box trainer and move and position it around from the designated starting point at point 1 and ending at point 10. After the surgeon completes the task, they are asked to report their opinions regarding maneuverability and perceived image quality.

2.3: Concept design

In the third phase of the context-driven design methodology, a convergent design approach is used, which is essential to assess various design options for effective laparoscopy. This involves the use of a morphological chart that delineates different methods by which each function of a laparoscope can be achieved, taking into account the size constraints set by the OmniVision 5693-based imaging system, as noted in Table 2.

Table 2: Dimensions of the OV5693 imaging system

Part	Dimensions
Sensor head	8.5x8.5x4.95mm
Ribbon cable	8x0.3x180mm
Processing board	30x15x3.6mm

The functions required for laparoscopic imaging encompass a range of actions that need to be performed by the laparoscope and surgeon. These functions begin with entering the scope into the body through a trocar to initiate the procedure. Once inside the abdomen, the laparoscope must be moved to target the diseased or inspection-required tissue. Next, the tip has to be oriented at 30 degrees since this is a crucial design feature.

Following the correct positioning and orientation of the distal end, it is essential to illuminate the tissue.

The illuminated tissue must be captured, and the reflected light must be focused on the sensors. These sensors convert the light into an electrical current, which is then processed into a video signal. Considering the scope's orientation to the outside world is crucial to minimize dissociative effects, particularly with a 30-degree angle offset. It necessitates understanding the image sensor orientation in relation to the horizon.

The comprehensive morphological assessment, presented in Appendix 2.1 and summarized text form in Table 2, examines each element involved in the function. The selection of specific parts for each conceptual design, as indicated by the numbers in Table 2, is based on strict adherence to functional requirements. A set of 6 concepts was designed to cover the chart's entire design space.

Options that did not comply with the hard requirements were excluded from all concepts, as noted further in Appendix 2.2.

Table 3: Morphological chart in text form with numbers linking to concepts

Entering the body	Rigid uniform outer diameter shaft (1, 2, 3)	Rigid varying outer diameter shaft	Flexible uniform outer diameter shaft (4)	Flexible varying outer diameter shaft (6)	Folding or assembling the shaft (5)
Maneuvering of the tip to the tissue	Rigid body motion (1, 2, 3, 5, 6)	Passive joint movement (4)	Motor actuated movement		
Orientation of the tip to the tissue	Rigid body motion (1, 6)	Multi-body motion (2, 3)	Compliant (4, 5)	Shape memory alloy	Microfluids mechanism
Light generation	External source (2)	Light emitting shaft	Parallel to the tip (2, 3, 4, 5, 6)	Passing through the scope (1)	
Light focusing on the sensor	The light is focused at the tip (2, 4, 5, 6)	The light is focused further in the shaft (3)	The light is focused outside the body (1)		
Global orientation of the laparoscope	Physical indication points on scope (2, 4, 5)	Optical correction (1, 3)	Software correction based on sensors (6)		

2.3.1: Concept 1: The Light head scope

The first concept, the light head laparoscope, depicted in Figure 3 with corresponding annotations, is designed with a camera head that integrates a light source (A), connected to a conventional slender scope featuring a 30-degree angle offset (B). This scope is connected to the head via a C-mount (C), ensuring that the lens is securely fastened and the image sensor is aligned with the lenses. Light transmission is achieved through a short optical fiber cable (D) from the light source in the handle, which interfaces with the optical fibers within the scope to deliver illumination to the distal end.

The Global orientation of the scope tip is maintained through the rotation of the lens within the C-mount. This design maintains the global orientation during

manipulation. A notable distinction in design compared to traditional laparoscope heads is the inclusion of the light source within the handle.
This integration reduces the necessity for a long optical fiber cable and a separate light source within the laparoscopic tower. Therefore, the system is streamlined to require only the camera head, the slender scope, and a laptop to facilitate laparoscopic imaging.

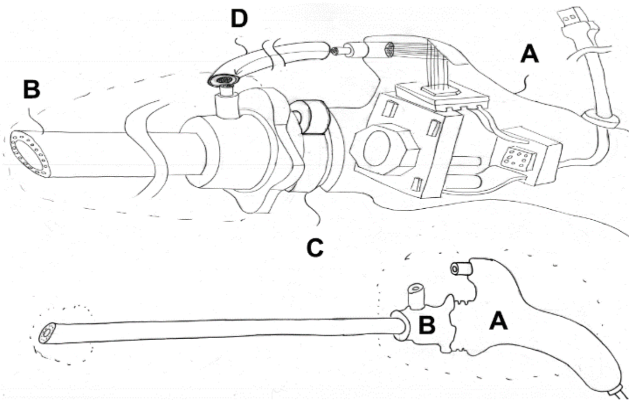

Figure 3: Concept drawing with annotations of the light head

2.3.2: Concept 2: The Unity laparoscope

The second concept, the unity laparoscope, illustrated in Figure 4 with corresponding annotations, features a single-piece rigid laparoscope. The design incorporates image sensors and LED lights at the tip of the scope (A), which is angled at 30 degrees. The data from these image sensors is transmitted through a ribbon cable to the laparoscope's handle (B), where it is processed. Additionally, the handle houses the components that regulate the wattage of the LED lights, ensuring efficient operation (C).

The laparoscope's handle is designed to be straight (D), requiring the entire scope to be rotated for tip FOV adjustments. The global orientation is noted by a bump located at the 12 o'clock position on the handle (E). This provides the surgeon with a tactile reference for the orientation of the tip during surgery.

For enhanced tissue illumination and possible lower tip temperatures, the system utilizes an external light source (F), which could be a lift device with light in the gasless use case. Integrating internal lighting and image sensors at the tip negates the need for an elongated lens and complex internal light transmission mechanisms. The streamlined design requires only the laparoscope itself, a possible external light source for additional illumination, and a laptop to facilitate laparoscopic imaging.

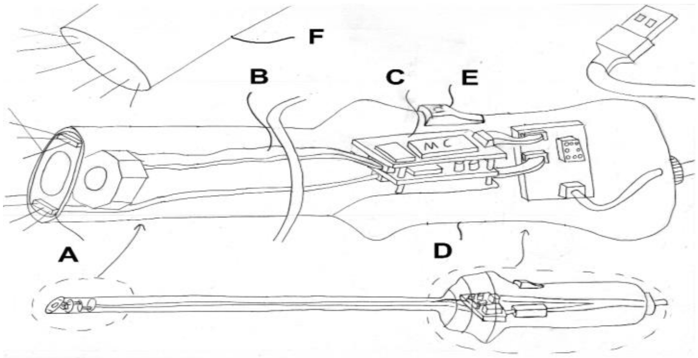

Figure 4: Concept drawing with annotations of the Unity laparoscope

2.3.3: Concept 3: The Rotary laparoscope

The third concept, the rotary laparoscope, illustrated in Figure 5 with corresponding annotations, combines elements from previous concepts. The sensor is mounted straight within a shaft (A) encased by a rotatable outer shaft (B). This outer shaft houses a series of lenses and a prism designed to focus and establish a 30-degree viewing angle (C). A set of LEDs integrated within the outer shaft (D) illuminate the tissue.

The visual information captured by the sensor is relayed via a ribbon cable to the handle, where image data is processed, and the power for the LEDs is regulated for efficient operation(E). The design requires rotary contact to supply power to the LEDs, effectively preventing cable damage from twisting motions.

This concept minimizes the use of lenses compared to the beam head scope by situating the image sensor proximal to the scope's tip but maintaining the ability to rotate the scope separately from the handle. Consequently, the system demands only the laparoscope and a laptop to facilitate laparoscopic imaging.

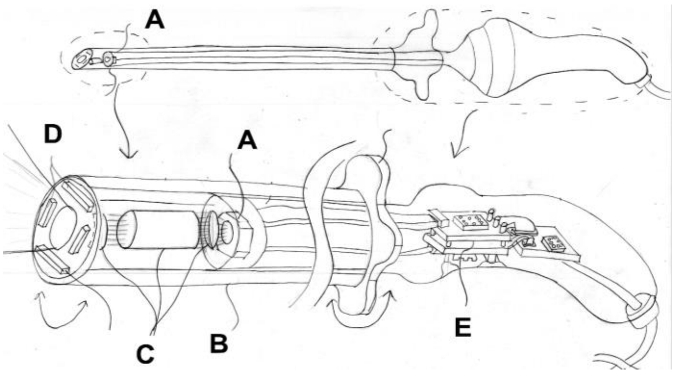

Figure 5: Concept drawing with annotations of the Rotary laparoscope

2.3.4: Concept 4: The FlexEye laparoscope

The fourth concept, named the FlexEye laparoscope and depicted in Figure 6 with corresponding letters, introduces an innovative orientation mechanism for the image sensor. The scope uses a flexible section with a nitinol-compliant backbone (A) that bends when a moment is applied at the top of the section by a wire, which runs through the scope's length. This wire is anchored at the back end of the laparoscope to a similar flexible component (B), which sets the orientation of the scope's tip to a 30-degree angle when no force is applied. The bending part is designed to form a uniform, slender tube at the tip to facilitate insertion through a trocar when force is applied to the bending section at the back of the scope.

Next to the image sensor, which is oriented at a 90-degree angle from the tip, a set of LEDs (C) is integrated to provide necessary illumination to the operative field. The captured data is transmitted through a ribbon cable to the handle, where the image is processed, and the LED power is regulated to ensure optimal performance (D). The scope's handle has a straight form and needs to be rotated to adjust the tip's FOV. A tactile bump positioned at the 12 o'clock mark on the handle (E) serves as a global orientation indicator, allowing the surgeon to determine the global orientation of the scope. The FlexEye scope requires only the laparoscope itself and a laptop to facilitate laparoscopic imaging, streamlining the surgical process and equipment needs.

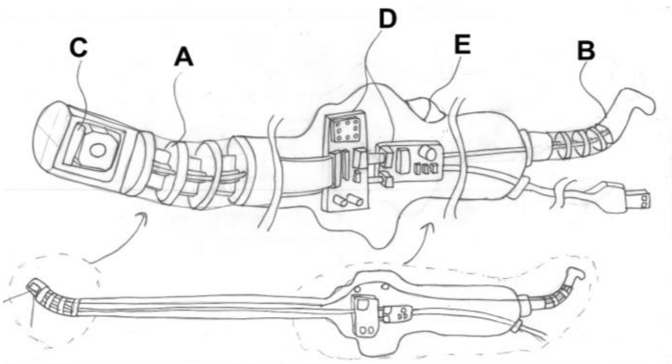

Figure 6: Concept drawing with annotations of the FlexEye laparoscope.

2.3.5: Concept 5: The Flip laparoscope

The fifth concept, named the Flip laparoscope, illustrated in Figure 7 with corresponding annotations, adopts a mechanism akin to that of the FlexEye concept, featuring a flexible tip that changes the orientation of the imaging sensor. The sensor is set at a 60-degree orientation, allowing for an expanded space for the sensor head. It is further rotated by an additional 30 degrees using a torsion spring (A), positioning the imaging sensor at the 30-degree viewing angle.

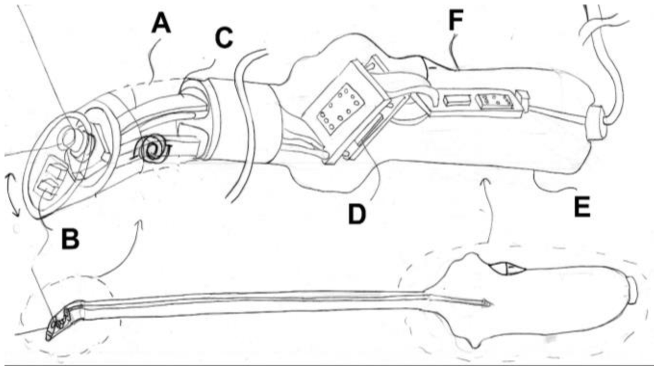

Figure 7: Concept drawing with annotations of the Fold laparoscope.

The scope’s tip can be adjusted by applying a force at the tip, straightening it out for trocar entry. During insertion, the tip can be straightened by pressing it against the inside of the trocar. Upon exiting the abdomen, the tip is designed to fold back into a straight position when pulled up, aligning with the uniform shaft for removal.

A set of LEDs (B) illuminating the tissue is integrated adjacent to the sensors at the tip. The visual data captured by the sensors is transmitted via a ribbon cable to the handle (C), where image processing happens, and the LED wattage is controlled for optimal performance (D). The laparoscope's handle is kept straight (E), a design choice that necessitates the rotation of the entire instrument to adjust the tip orientation. A tactile indicator, in the form of a bump at the 12 o'clock position on the handle (F), allows the surgeon to understand the global orientation of the tip. This concept ensures that laparoscopic imaging requirements can be performed with just the laparoscope and a laptop.

2.3.6: Concept 6: The Stretch laparoscope

The final concept, the Stretch laparoscope, depicted in Figure 8 with annotated letters, introduces a design inspired by an alternative laparoscopic entry technique that involves stretching rather than further incising the skin. This approach necessitates a specialized trocar designed for gas laparoscopy, featuring a flexible inner layer that can accommodate the rigid, non-uniform shaft of the laparoscope during entry.

At the forefront of the device, the image sensor is positioned within a beveled tip set at a 30-degree angle (A). Adjacent to the sensor, LED lighting is integrated to provide the necessary illumination (B). Visual data captured by the sensor is conveyed along a ribbon cable to the handle, where it undergoes processing (C), and the LED wattage is controlled for optimal performance (D).

The laparoscope's handle is straight (E), a design choice that necessitates the rotation of the entire instrument to adjust the tip FOV. An innovative aspect of this concept is the software-based image orientation correction facilitated by an accelerometer and a microcomputer integrated within the handle (F). These components work together to determine the global orientation of the scope, allowing the displayed image to include an arrow that indicates orientation relative to the patient. This concept ensures that laparoscopic imaging requirements can performed with just the laparoscope, flexible trocar, and a laptop.

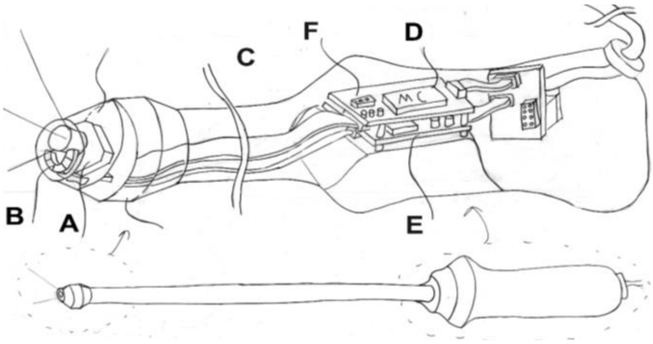

Figure 8: Concept drawing with annotations of the Fold laparoscope.

2.3.7: Concept validation

The selection of a final design for the laparoscope was performed by utilizing the Harris profile methodology. The concepts were tested based on cost, invasiveness, robustness, reprocessability, serviceability, and compatibility and scored based on their performance. The rating for each concept based on the performance criteria is further elaborated upon in Appendix 2.3.

After assigning scores to each concept across all criteria:

- Concepts 4 and 5 emerged as the leading candidates due to their balanced attributes in cost-efficiency, minimal invasiveness, robustness, ease of reprocessing, and serviceability. They also displayed reasonable compatibility with current surgical equipment based on their shaft diameter.

- Concept 2 was noted for its cost-effectiveness and simplicity of design.

- Concept 1 showed high compatibility with existing surgical instruments but fell short on cost and robustness.

Based on the functional and performance requirements for designing a laparoscope for low-income settings, it was found, based on the Harris profile as shown in Table 4, that concepts 4 and 5 are the most promising concepts. These concepts will be prototyped to validate the effectiveness and optimize the design.

2.3.8: Functional prototypes

Based on the results of the Harris profile, the two most promising concepts were prototyped using off-the-shelf electronics, plastics, and 3d printed parts, as shown in Figure 9. For simplicity in construction, the prototypes utilized tubes with a 12mm diameter. The functionality of the prototypes was demonstrated using a makeshift box trainer setup, which provided an external user view and internal view of the box and the scope's operation. A link to these video demonstrations is available in Appendix 2.4.

Figure 9: Intermediate prototypes of FlexEye laparoscope (bottom) and the Flip laparoscope (bottom)

Table 4: Harris profile assessment of the six concepts based on the performance criteria.

	Weight	Concept 1	Concept 2	Concept 3	Concept 4	Concept 5	Concept 6
Cost	10p	1 * 10	5 * 10	2 * 10	4 * 10	4 * 10	5 * 10
Invasiveness	10p	5 * 10	2 * 10	1 * 10	4 * 10.	3 * 10	1 * 10
Robustness	10p	1 * 10	4 * 10	2 * 10	4 * 10	4 * 10	4 * 10
Ease of reprocessabity	7p	3 * 7	5 * 7	3 * 7	4 * 7	4 * 7	5 * 7
Serviceability	4p	1 * 4	2 * 4	3 * 4	3 * 4	3 * 4	2 * 4
Compatibility	3p	5 * 3	2 * 3	2 * 3	4 * 3	4 * 3	1 * 3
Total score		**110**	**159**	**94**	**172**	**162**	**145**

During testing, the prototype derived from FlexEye concept encountered issues with achieving a uniform diameter along the shaft due to slack in the control cable and friction encountered by the cable within the bending elements.

These problems constrained the movement of the bending mechanisms to straighten the tip entirely. A larger-scale model of the mechanism was constructed to address and further investigate these issues to optimize the design given in Appendix 2.5.

The prototype based on Flip concept functioned as intended; however, there were concerns about potential friction and subsequent wear when interacting with the trocar used in the makeshift trainer. Such wear could adversely affect the trocar over time, which is undesirable.

After developing the prototypes, feedback was received from a direct end-user, laparoscopic surgeon Dr. J. Gnanaraj. This feedback was essential in refining the design and assessing its practical applications. The input regarding gas laparoscopy confirmed that smaller diameters are preferred, but a 12mm shaft would be perfectly acceptable, especially in regions where laparoscopy is not yet available.

In the case of gasless laparoscopy, where the constraints of trocar passage do not apply, the market potential for such an innovative laparoscope was recognized to be significant. Diverging the designs into two versions, one for gas and one for gasless laparoscopy, could have the most significant impact.

2.4: Final Design

2.4.1: Overview

Based on the Harris profile evaluation, prototype testing, and feedback from a laparoscopic surgeon, the design process's coming together has resulted in a final modular laparoscope called the FlexMod laparoscope. This design synthesizes the most successful elements of the FlexEye concept and takes inspiration from the Stretch concept for the gasless-specific use case, creating a versatile system that accommodates both gas and gasless laparoscopic procedures with the change of some components.

The basis of the design's modularity lies in the electronics and the handle, which are the universal components for both variants of the laparoscope. The handle contains the video processor and a custom circuit that manages the distribution of signals and power to both the video processor and the LED light transformer.

The modularity extends to the interchangeable parts, as illustrated in Figure 10, including a fully assembled gasless laparoscope noted with a B and the interchangeable parts needed to convert the laparoscope to the gas version with a straight shaft noted with an A. Overall, the shaft, the tip assembly, and the end part allow for the construction of different gas and gasless models.

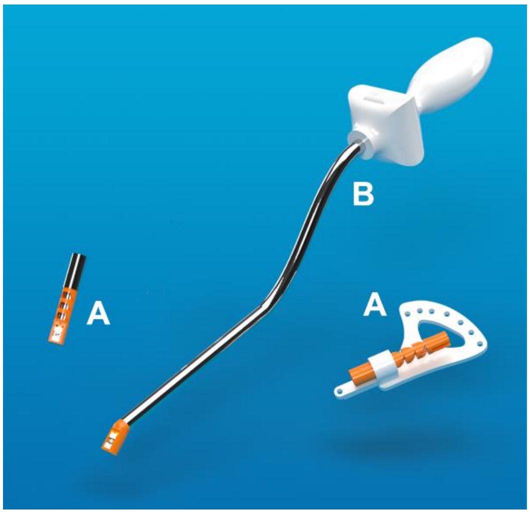

Figure 10: The FlexMod laparoscope, including interchangeable parts.

The tip of each modular unit is equipped with a custom OmniVision 5693 imaging system, details of which are elaborated in Appendix 2.6. The lighting is provided by three LEDs that operate at 3.3 volts and 400 milliamperes (mA). These LEDs are configured in parallel and emit a light temperature of 6000k, comparable to the illumination provided by commercial Xenon light sources[19]. The LEDs are housed in a circuit designed around the sensor's lens to optimize the tip size.

The LEDs and image sensors are shielded using Grillamid sheets that cover the tips. These sheets offer high optical clarity and durability and are certified with the use of disinfectants. The connection between the tip housing and the Grillamid covering is secured with epoxy glue, creating a watertight seal. This sealing ensures that the design can withstand reprocessing, meeting the requirements for HLD using OPA and glutaraldehyde solutions.

The handles and other minor components of the scope are constructed using 3D printing technology with ABS plastic, chosen for its compatibility with sterilizing agents and general use in medical instruments. The shafts are constructed from 316L medical stainless steel and the bending sections are sealed with medical shrink wrap which is constructed from polyolefin. Each variant of the modular design is discussed in detail in their respective sections, which include attention to the individual sections, function, and assembly.

2.4.2: Laparoscope for gas laparoscopy

The design for the gas laparoscope has been refined based on the feedback on the initial prototype testing of FlexEye Concept. This design iteration addresses the previous challenges of straightening the tip to fit through the trocar through an improved bending mechanism. Additional parts, such as a back, can hold the back bending section to set the tip to a viewing angle that is not only 30 degrees. The total design is made up of 4 sections, as illustrated in Figure 11: the tip (A), the shaft (B), the handle (C), and the back (D), with a total of 36 components.

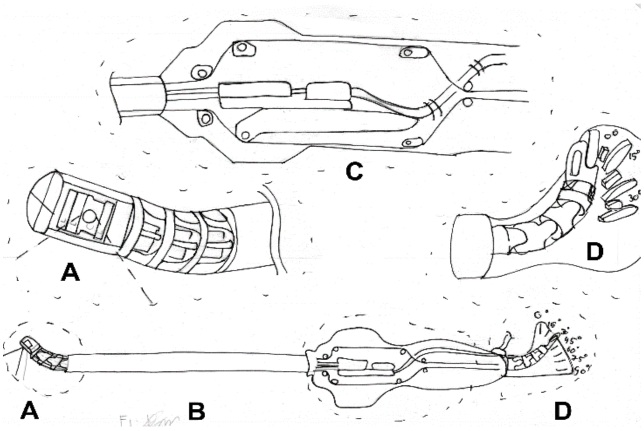

Figure 11: Drawings of the laparoscope version for gas laparoscopy with annotations relating to specific sections

Tip and Bending Mechanism

The modified bending design incorporates a centrally located nitinol strip, with dual cables at either side that extend or contract in response to the bending section's orientation at the back of the laparoscope. This change allows for more precise control over the tip's angle and eliminates the problem with slack encountered in prior prototypes.

As shown in Figure 12 with annotated letters, the tip and bending section assembly is designed to house the LED circuit (A) and image sensor (B) and is covered with a sheet. The tip with the sensor (C) slides into the top of the bending section (D); the bending section has a 0.4mm diameter nitinol wire (E) running through all elements of the bending section, ending in the element connected with the shaft (F). Adjacent to this compliant wire in the non-bending direction, electrical wires are run alongside (G), and a ribbon cable runs behind it, connecting to the image sensors (H). This configuration is strategically placed to reduce stress on the connectors during the bending motion. Above the bending section, the 0.5mm 314 stainless steel cables can be connected (I), which are tightened and threaded through the holes of the bending elements (J).

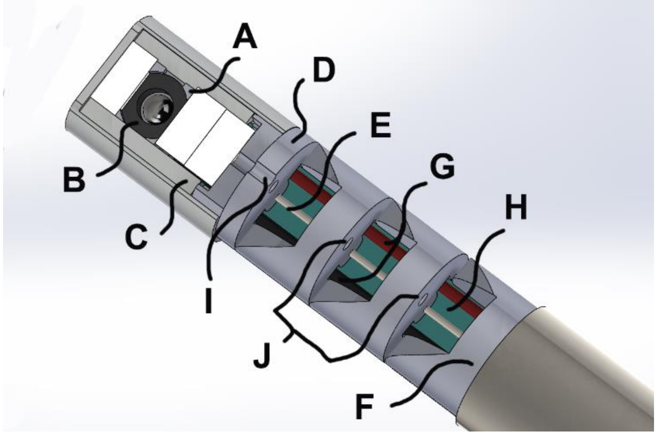

Figure 12: Tip and bending assembly with annotated letters noting specific parts and components

Shaft and handle

The cables originating beneath the image sensors and LED circuit traverse the shaft length together with the ribbon cable and LED power cables. As shown in the opened prototype in Figure 13 with annotated letters, the 12mm shaft enters the handle (A), connecting the tip to the body. These enter the handle where the ribbon cable interfaces with the image processor (B), translating the captured imagery into a JPEG USB video signal. The design ensures the steel cables are routed over and under posts (C) within the handle to eliminate contact with the processing board and damage. The LED power cables run underneath the processor, connecting to the power and transformer circuit (D) to step down the voltage from 5V to 3.3V and limit the current for the LED lights to reduce excess heat.

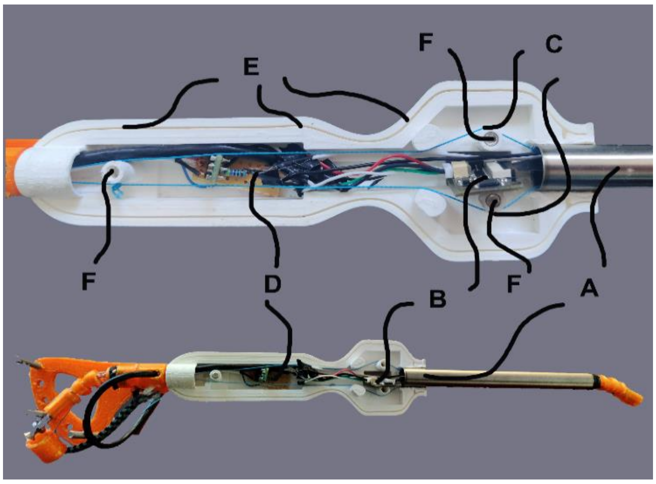

Figure 13: Prototype of the gas laparoscope with annotated letters relating to specific parts and components

Back section

The cables run through the back of the scope and through an identical bending section as found at the tip. The bending section ends in an end clamping part that can be placed at particular angles on the back plate, which is added to the back of the handle.

The Cables are secured via clamping and further tightened by a screw mechanism inside the clamping end part.

Assembly and Sealing

The internal components assembly is completed upon connecting the wires, ribbon cable and securing the cables. The bending sections are glued to the shaft and back part, which in turn is sealed with the handle using epoxy glue. The bending sections are encapsulated with medical polyolefin elastic shrink wrap. When all components except the handle are secured, the top handle piece can be placed on top of the bottom handle, which encloses the electronics and cable guides. A small gasket and epoxy glue within a groove and the surface along the handle's perimeter, as shown in Figure 12 (E), ensures a seal when compressed by a protruding feature from the top section of the handle when bolted together with three bolts (F) with a sealant applied to the bolt threads to prevent dust and liquid from entering. A slot at the rear of the handle allows for the securing and tightening of the back component, and USB wires are routed and sealed to prevent damage to the PCB connectors, contributing to the integrity and one-piece design of the laparoscope.

2.4.3: Laparoscope for gasless laparoscopy

The design for the gasless laparoscope incorporates the same handle and electronics as its gas counterpart, but it differs in shaft geometries, the tip, and the back part of the scope for the specific needs of gasless laparoscopic procedures. The total design is made up of 4 sections, as shown in Figure 14, with the prototypes: the tip(A), the shaft(B), the handle(C), and the back(D), with a total of 22 components.
The shaft variations are designed based on the end users' input, focusing on the ergonomics and functionality required for multi-incision and single-incision gasless laparoscopic surgery (SILS).

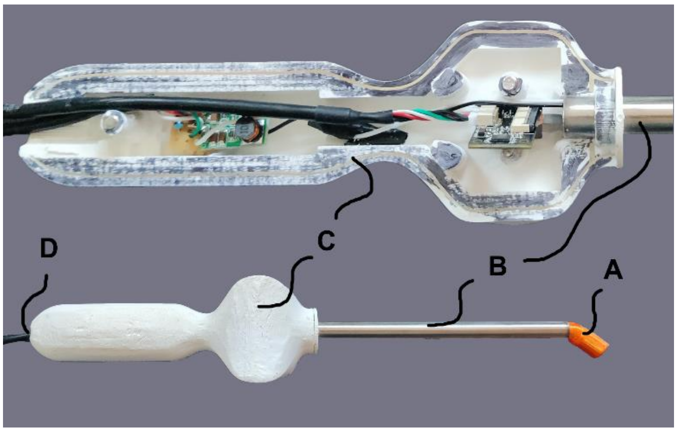

Figure 14: Prototype of the gas laparoscope with annotated letters relating to specific sections

Tip Section

In the gasless design, the tip is designed to be permanently bent to set the image sensor at a 30-degree angle, as shown in Figure 15 with annotated letters. The image sensor, along with its ribbon cable and power cables, are slit into the back tip section (A), which then connects to the shaft (B). Once the sensor is positioned, the top part of the tip (C), which houses the LEDs (D) on a circuit, is secured over the sensor (E) and covered with a sheet of Gillamid. The components are held together by friction and sealed with epoxy glue.

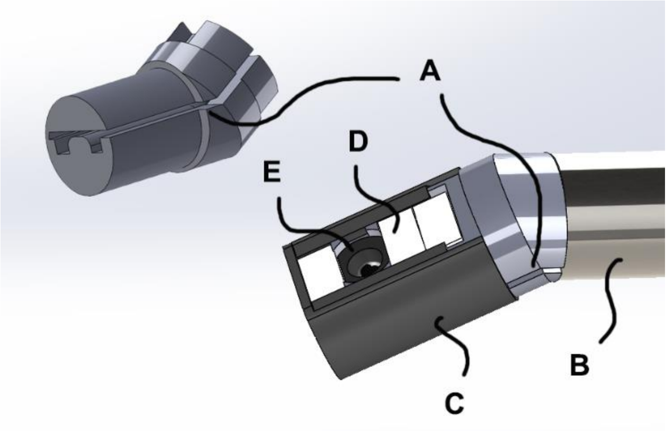

Figure 15: Tip and assembly of the gasless laparoscope with annotated letters noting specific parts and components.

Shaft, handle, and back section

The ribbon cable from the image sensor and the power cables of the LED are inserted through the 10mm shaft, guiding them toward the handle's electronic components. The gasless laparoscope features two shaft designs, as depicted in Figure 16. The first is a bent shaft optimized for SILS; the bend in the rod ensures that other instruments do not collide with the laparoscope handle when in the same entry hole. The second design is a straight shaft, which is traditional and suitable for multi-incision gasless laparoscopy.

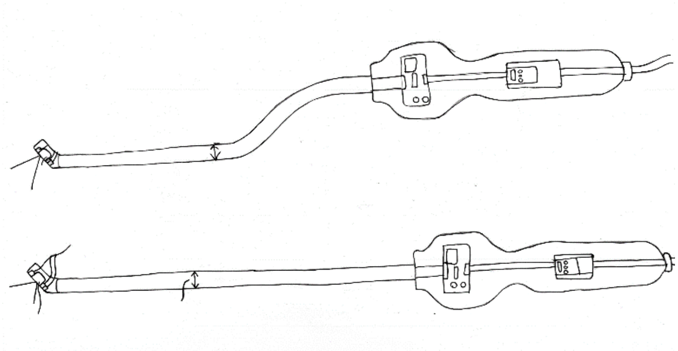

Figure 16: Drawings of two different shafts for the gasless laparoscope

Similar to the gas laparoscope, the ribbon, and LED power cables exit the handle, connecting to the image processor and power circuit in the handle. At the rear of the handle, the outgoing USB cable connected to the power circuit and image processor is clamped and routed outside the laparoscope.

Assembly and Sealing

Assembly of the laparoscope follows the same procedure as the gas version, ensuring all cables are connected, the shaft and tip are glued into place, the USB cable is secured, and the handle is sealed with bolts and epoxy glue. Resulting in a completely sealed one-piece design.

2.4.4: Displaying of the image and features.

The first part of this study found that the displaying software significantly influences the image quality of USB camera systems. The study suggests using the software Resolume Avenue until specific software is developed. Resolume Avenue is now set up with panning and zooming with a range of 100% to 250%, mapped to keyboard controls.

2.4.5: Measurement results

Weight Analysis

Commercial laparoscopes typically weigh between 1-2 kg, with a significant portion of this weight coming from the slender scope. For ease of use, especially during extended procedures, the new laparoscope designs must be equal to or lighter than this standard. After testing, the gas and gasless laparoscope prototypes were found to be significantly lighter, with the gas design weighing 229 grams and the gasless design at 188 grams.

Cost Analysis

The costs of the gas and gasless laparoscope prototypes are covered in Table 5 and explained in detail in Appendix 2.7. These costs vary depending on the production scale, particularly for components that are custom-made.

The table presents a breakdown of costs for individual and larger-scale (indicated by '>50') productions. In large-scale production, the cost of imaging components significantly decreases. However, for single- or large-scale production, the cost will be well below the threshold of 500 euros, meeting the cost requirements for the laparoscopes.

Table 5: Cost overview for both versions of the laparoscopes

	Gas (1)	Gas (50>)	Gasless (1)	Gasless (50>)
Imaging and light	€92.39	€41.13	€92.39	€41.13
Shaft	€17.22	€12.73	€11.48	€7.65
3d printed handle	€2.76	€2.76	€2.76	€2.76
Other mechanical parts	€2.54	€2.54	€0.11	€0.11
Other electrical parts	€8.02	€8.02	€8.02	€8.02
Sealants	€1.75	€1.75	€1.75	€1.75
Total	€123.96	€67.72	€115.88	€66.09

Illumination

The required amount of illumination was determined based on the number of lumens the selected LED lights produced. The selected LEDs advertise 100 lumens for a 3.3V, 150mA LED light. The required minimum of 2200 lux is obtained at 100mm with a light source of about 275 lumens. Two designs were tested with 2 LEDs and one with 3 LEDs run at 3.3v at 300mA and 400mA; the results are in Table 6. The Table shows that the three LEDs exceed the required quantity at 50 mm but fall short at 100mm, and the two LEDs do not reach the necessary amount of lux at either distance.

Table 6: light intensity in lux measurements at different operational distances

	distance	Intensity
Three lights	100mm	1350 lux
	50mm	3280 lux
Two lights	100mm	870 lux
	50mm	2100 lux

Thermal Measurement

The final design variant for the gasless laparoscope underwent a thermal measurement test of 180 minutes. The results of this test, as shown in Figure 17, show that the temperature of both the shaft and the handle remained below body temperature throughout the testing period. The tip of the laparoscope settled at a temperature of around 46 degrees Celsius. This temperature is below the safety threshold of 48 degrees Celsius for constant exposure, and the higher safety limit of 56 degrees Celsius is designated for shorter exposure times of up to one minute. This implies that the whole laparoscope could safely remain in contact with tissue for extended periods without posing a risk of burns.

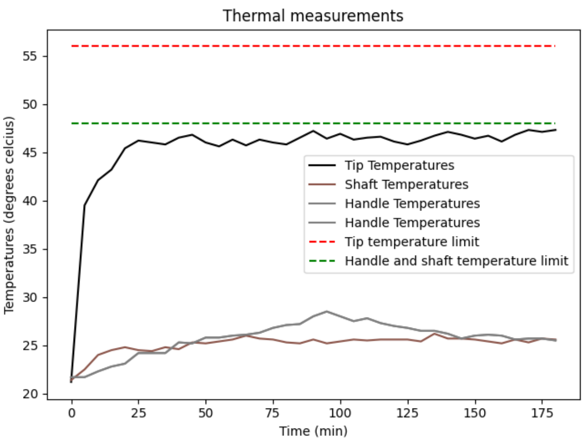

Figure 17: Thermal measurement results for the final prototype.

Reprocessing

The gasless laparoscope design was tested for its ability to be reprocessed using chemical sterilizing agents. Each component of the laparoscope, the tip, handle, and shaft, was submerged separately in a water tank for one hour to simulate this process. Using only the gasket and minor amount off epoxy glue, the design cannot seal the handles effectively. However, when combined with epoxy glue around the whole contact area between the handles, positive results were found. The results for the tip and shaft were also positive, as no leaks were discovered after an hour of submerging the tip, and shaft.

User-test

On November 20th, a user test involving the laparoscope prototypes was conducted in the MISIT lab with Dr. J. Gnanaraj, a laparoscopic surgeon. The test utilized prototypes with a shorter shaft of 150mm since the custom imaging system had not yet been produced. During this session, as shown in Figure 18, the surgeon provided insightful feedback on both the gas and gasless laparoscope designs by performing the set-out task.

The laparoscopic surgeon noted that the image quality and illumination were excellent for the gas laparoscope, comparable to the state-of-the-art. However, he raised concerns about the design's complexity and its market adoption potential. He suggested that surgeons who are accustomed to using well-established, professional equipment might be reluctant to switch to a new, less-known device.

His response to the gasless laparoscope was significantly more positive. He was particularly impressed with its rigidness and simplicity Dr. J. Gnanaraj stated, “This scope could revolutionize laparoscopy in sub-Saharan Africa.” Furthermore, the surgeon offered further design suggestions for the gasless laparoscope for future design improvements, explained further in Appendix 2.8.

Figure 18: Laparoscopic surgeon testing laparoscope prototypes in the MISIT lab.

2.5: Discussion

The primary goal of this study was to design a low-cost laparoscope based on the findings of the first part of this thesis. A modular design for two different use cases was created and prototyped to be tested.

The tests showed promising results, though certain factors in the methods, design process, and testing may have limited or affected the results of this study.

2.5.1: Methods

The initial phases of the roadmap involved end user input exclusively from Dr. J. Gnanaraj, a surgeon based in India with expertise in rural and gasless laparoscopic surgery. His experience, though invaluable, might have introduced certain biases in the design requirements for the laparoscope. This potential bias could limit the use of the design to other settings.

The list of functions in the morphological chart aimed to cover the required processes to enter the laparoscope in the abdomen and obtain both traditional and gasless laparoscopy. The gasless laparoscope would require fewer functions for visualizing the abdomen of the abdominal region size, it does not have to fit through a trocar to reach the inside of the abdomen. This reduction in requirements could have resulted in a loss of potential design space, potentially leading to missed opportunities for innovative design solutions for the gasless laparoscope.

The design space was constrained based on the size of the OV5693 imaging system components. The dimensions of the processing board, in particular, impose a constraint, requiring its placement exclusively in the handle of the device. To fulfill the ability to fit through a trocar and the length of a tip from handle requirement.

2.5.2: Final design prototypes

The materials selected for the laparoscopes are designed to withstand chemical disinfection agents and are suitable for surgical use. However, the Fused Deposition Molding (FDM) 3D printing method used for production has a chance of potentially leaving tiny cavities between layers, which could cause leaks. This requires the validation of each part which comes in contact with the disinfecting agents. Switching to injection molding could offer a more reliable alternative for larger-scale production.

The prototypes required the use of two USB cables because a single USB 2 connection could not support the current draw from the transformer and image processor. The solutions to this issue could be using a 6-pole shielded cable with dual USB 2 connectors or switching to a USB 3 connector, which can supply higher currents.

2.5.3: Final design measurements

The design includes a silicone gasket around the perimeter of the handle to open the handle for repairs. However, it was found in the reprocessing test that the gasket and epoxy glue in the cavity and outside layer itself did not completely seal the handle. Therefore, the sealing of the whole contact area of the handles with epoxy glue was required, which resulted in positive results. Reducing the ability to be serviced when a component breaks without breaking the handle. However, Sealing the device completely offers the advantage of preventing the chance of incorrect sealing due to the silicone gasket.

In estimating the cost of larger-scale production, the prices of some components were not directly available. Therefore, single-use prices were used for these calculations. However, the actual costs in mass production would likely be lower, leading to an estimated price point for the laparoscopes around 50 euros. It's important to note that this cost estimation is based only on component prices and does not include the used machinery, electricity or assembly costs.

Regarding the weight of the prototypes, measurements were taken with 150mm shafts, which reduced the overall weight compared to the 300mm shaft. A shaft with a 10mm outer diameter and a 9mm inner diameter, measuring 300mm in length and made of 314 stainless steel, was measured to weigh 30 grams. This material differs from the intended 316L stainless steel, but the densities of both materials are similar, with 314 having a density of 7,900kg/m^3 and 316L 8,000kg/m^3 at 20 degrees Celsius. Therefore, this slight difference in material density is does not impact the overall weight of the laparoscope significantly.

User testing of the gasless laparoscope proved successful even with the shorter imaging system and shaft of 150mm. However, the handle was near the entry hole which would be a problem for SILS and the general ergonomics of holding the device. For this reason, a longer shaft and custom imaging system with ribbon cable length of 300mm is required for future prototypes.

2.5.4: Future research

In the thermal measurement tests using a box trainer, the ambient temperature was 21 degrees Celsius, significantly lower than the typical abdominal body temperature. This discrepancy could influence the settling temperatures of the laparoscope's shaft and tip. Future studies should aim to replicate these tests under conditions that more accurately mimic the in-body environment to assess the temperature of the laparoscope.

The advised software to display the image is where the bulk of the cost is. In order to reduce the cost of the laparoscope, future development should focus on creating stable, non-compressing software with similar features regarding input video sources as Resolume Avenue.

The laparoscope encountered glare reflection from the Grillamid sheet on the image sensor due to the LEDs, indicating that the Grillamid sheet used lacks an anti reflective coating or is not sufficiently optically clear or thick. The sheet supplied for testing was 2 mm thick and was not coated with anti-glare coating. The problem could be resolved by separating the image sensor from the LEDs, though it may result in a longer tip. Future research should explore alternative materials and the influence of thickness and coatings for better optical clarity.

The LED light current had to be constrained since it would exceed 60 degrees Celsius at their operating voltage and current in a few seconds. The advertised amount of light production also does not match the measured intensity. Further research should be performed to test different LEDs and their performance. To eliminate the possibility of reflective glare from the tissue when the light intensity is improved, the ability to dim the light could prove vital and should, therefore, be included in further development.

Issues were encountered with the cable tension and flexibility of the heat shrink at the tip and back of the device. The initial plan to use elastic medical shrink wrap was abandoned due to the difficulty and cost of acquiring test samples. Instead, a readily available flexible heat shrink made of the same material was used, but it resulted in the design becoming too stiff after only a few degrees of bending.

Further research is required to explore more suitable flexible heat shrink materials that are used on endoscopes.

The device's lifespan has not been determined as of this phase of development of the laparoscope. Ideally, they could be used daily for extended periods of time. Though no testing regarding this aspect has been conducted, future research is required to determine the durability of the laparoscope.

2.6: Conclusion

This study aimed to design and validate a low-cost laparoscope based on the findings of the first part of this thesis, which compared low-cost imaging systems to state-of-the-art commercial laparoscopes. To select the most comparable imaging system and define the required illumination. Following the first part, a design approach based on 'Roadmap for Design of Surgical Equipment for Safe Surgery Worldwide' is employed. The roadmap's first phases combine the requirements from end users and literature in a comprehensive list of requirements used for a context-driven design.

The context design process led to the creation of a modular laparoscope adaptable for both gas and gasless laparoscopy. With its reduced complexity compared to the gas laparoscope in terms of required parts and assembly, the gasless version was praised by a renowned laparoscopic surgeon, who was impressed with its image quality and design. Both laparoscope versions could significantly impact laparoscopy in low-income counties and rural settings in India and sub-Saharan Africa. However, some areas require further research to address this study's limitations regarding materials and real-world surgical conditions.

In summary, this thesis has compared various image systems to those used in commercial laparoscopes, leading to the selection of a suitable imaging system for our low-cost laparoscope. Following the roadmap, several concepts were created and rated, coming together in a modular final design. The gasless laparoscope has captured the interest of the Indian surgeon for future development to promote gasless laparoscopic surgery as a cost-efficient alternative to conventional laparoscopy, which could significantly increase access to laparoscopy to those who could gain the most from it.

2.7: References

[1] A. Buia, F. Stockhausen and E. Hanisch, "Laparoscopic surgery: A qualified systematic review," *World Journal of Methodology,* vol. 5, no. 4, p. 238, 2015.

[2] R. Garry, "Laparoscopic surgery," *Best Practice and Research: Clinical Obstetrics and ,* vol. 20, no. 1, pp. 89-104, 2006.

[3] J. Shen, J. Zhang, C. Huang, ""Clinical comparison of laparoscopy vs open surgery in a radical operation for rectal cancer: A retrospective casecontrol study," *World Journal of Gastroenterology,* vol. 21, pp. 13532-15341, 2015.

[4] A. Ternamian, J. Dempster, G. Vilos, "Laparoscopic Entry: A Review of Techniques, Technologies, And Complications," *Journal of Obstetrics and Gynaecology Canada,* vol. 29, no. 5, pp. 433-447, 2007.

[5] S. Krishnakumar, P. Tambe, "Entry Complications in Laparoscopic Surgery," *Journal of Gynecological Endoscopy and Surgery,* vol. 1, pp. 4-11, 2009.

[6] B. Smith, A Shih, S. Hohmann, N. Nguyen, "Use of laparoscopy in general surgical operations at academic centers," *Surgery for Obesity and Related Diseases,* vol. 9, no. 1, pp. 15-20, 2013.

[7] A. Taqdeer, R. Gosselin, S. Contini, "Should Laparoscopic Cholecystectomy be Practiced in the Developing World? The Experience of the First Training Program in Afghanistan," *Annals of Surgery,* vol. 251, no. 3, pp. 574-578, 2010.

[8] J. Kasai, M. Bruhat, J. Raiga, "Laparoscopic surgery in the Cameroon," *International Journal of Gynecology & Obstetrics,* vol. 65, no. 1, pp. 65-66, 1999.

[9] M. Mugford, Y. Teerawattana, "Is it worth offering a routine laparoscopic cholecystectomy in developing countries? A Thailand case study," *Cost Effective and Resource Allocations,* vol. 10, no. 3, pp. 3-10, 2005.

[10] D. Pizzol, M. Trott, I, Grabovac, M. Antunes, "Laparoscopy in Low-Income Countries: 10-Year Experience and Systematic Literature Review," *Int J Environ Res Public Health,* vol. 18, no. 11, 2021.

[11] N. el-Mattarid, M. Sief, S. Shamoun, E. Rypins, Y. Basha, "The first 100 laparoscopic cholecystectomies in the Republic of Yemen," *J Laparoendosc Surg,* vol. 5, no. 3, pp. 163-167, 1995.

[12] T. Udwadia, "Diagnostic laparoscopy," *Surg Endosc,* vol. 18, no. 1, pp. 6-10, 2004.

[13] O. Awotunde, A.ogunlaja,L. Olujide, O. Fehintola, "Preliminary report of experience with gynaecologic laparoscopy in Ogbomoso, Nigeria," *Gynecological Surgery,* vol. 13, pp. 17-21, 2016.

[14] G. Ahmad, D. Gent and D. Henderson, "Laparoscopic entry techniques," *Cochrane Database of Systematic Reviews,* 2015.

[15] R. Pickard,C. Robertson, A Close, C Ramsay, "Systematic Review and Economic Modelling of the Relative Clinical Benefit and Cost-Effectiveness of Laparoscopic Surgery and Robotic Surgery for Removal of the Prostate in Men with Localised Prostate Cancer", Southampton:

Health Technology Assessment, 2012.

[16] H. Ahmad, H. Khan, Awais Khan, O Tanoli, "Laparoscopy in Low- and Middle-Income Countries: A Survey Study," *Cureus,* vol. 15, no. 6, 2023.

[17] R. Oosting, L. Wauben, J. Madete, R. Groen, J. Dankelman, "Availability, procurement, training, usage, maintenance and complications of electrosurgical units and laparoscopic equipment in 12 African countries," *BJS Open,* vol. 4, no. 2, pp. 326-331, 2020.

[18] R. Mishra, Textbook of Practical Laparoscopic surgery, New Delhi: Jaypee brothers medical publisher LTD., 2013.

[19] D. Kruschinski, Atlas of lift-Laparoscopy, London: Informa UK Ltd, 2007.

[20] V. Paolucci, C. Gutt, B. scheaff, A. Encke "Gasless laparoscopy in abdominal surgery," *Surgical Endoscopy ,* vol. 9, pp. 497-500, 1995.

[21] I. Chatzipapa, N. Kathopoulis, A. Protopapas, D. Loutradis, "Using a Mobile Smartphone to Perform Laparoscopy," *Journal of Minimally Invasive Gynecology,* vol. 25, no. 5, pp. 912-915, 2018.

[22] J. Mueller, N. Rozman, E. Sunassee, A. Gupta, C. Schuval, "An Accessible Laparoscope for Surgery in Low- and Middle- Income Countries.," *Ann Biomed Eng,* vol. 49, no. 7, pp. 1657-1669, 2021.

[23] M. Gaab, "Instrumentation: endoscopes and equipment.," *World neurosurgery,* vol. 79, no. 2, pp. 11-21, 2013.

[24] R. Oosting, J. Dankelman, L. Wauben, "Roadmap for Design of Surgical Equipment for Safe Surgery Worldwide," *EEE Global Humanitarian Technology Conference,* pp. 18-21, 2018.

[25] A. Shushan, H. Mohamed, A. Magos, "How long does laparoscopic surgery really take? Lessons learned from 1000 operative laparoscopies," *Human Reproduction,* vol. 14, no. 1, pp. 39-43, 1999.

[26] Power Electronics, "Design Considerations for Maximum Allowable Temperature," Ventura, 2019.

[27] ASP CIDEX, "Technical information CIDEX OPA," Irvine, 2020.

[28] D. Zezo, "Laparoscopic/Robotic Camera and Lens Systems," Abdominal key, 2018.

[29] C. Garg, B. Vaidya, M. Chengalath, "Efficacy of laparoscopy in complicated appendicitis," *International Journal of Surgery,* vol. 7, no. 3, pp. 250-252, 2009.

[30] S. Lee, H. Kim, D. Sohn, J. Eom, "Indocyanine green-loaded injectable alginate hydrogel as a marker for precision cancer surgery," *Quant Imaging Med Surg,* vol. 10, no. 3, pp. 779-788, 2020.

Appendix 1.1: Vendor information and sourcing link

The four imaging systems were initially acquired to perform the test with two endoscopes and two smartphone-based imaging systems. However, the 7mm endoscope imaging system malfunctioned and ceased sending a signal.

Omnivison 5693 USB camera system vendor link: https://nl.aliexpress.com/item/1005004149480948.html?spm=a2g0o.order_list.order_list_main.221.1fc879d2qvhHKq&gatewayAdapt=glo2nld

Omnivison 9732 USB camera system vendor link:

3.9mm Endoscope Camera Module USB 720p for Android - Dothecamera

Sony IMX 258 USB camera system vendor link:

https://nl.aliexpress.com/item/1005003453515329.html?spm=a2g0o.order_list.order_list_main.216.1fc879d2qvhHKq&gatewayAdapt=glo2nld

7mm endoscope USB camera system vendor link:

https://nl.aliexpress.com/item/1005003453515329.html?spm=a2g0o.order_list.order_list_main.216.1fc879d2qvhHKq&gatewayAdapt=glo2nld

Appendix 2.1: Morphological Overview

the complete morphological overview with images, as shown in Figure A, displays the entire design space for the function. These functions need to be completed to visualize the abdominal region in gas and gasless laparoscopic surgery.

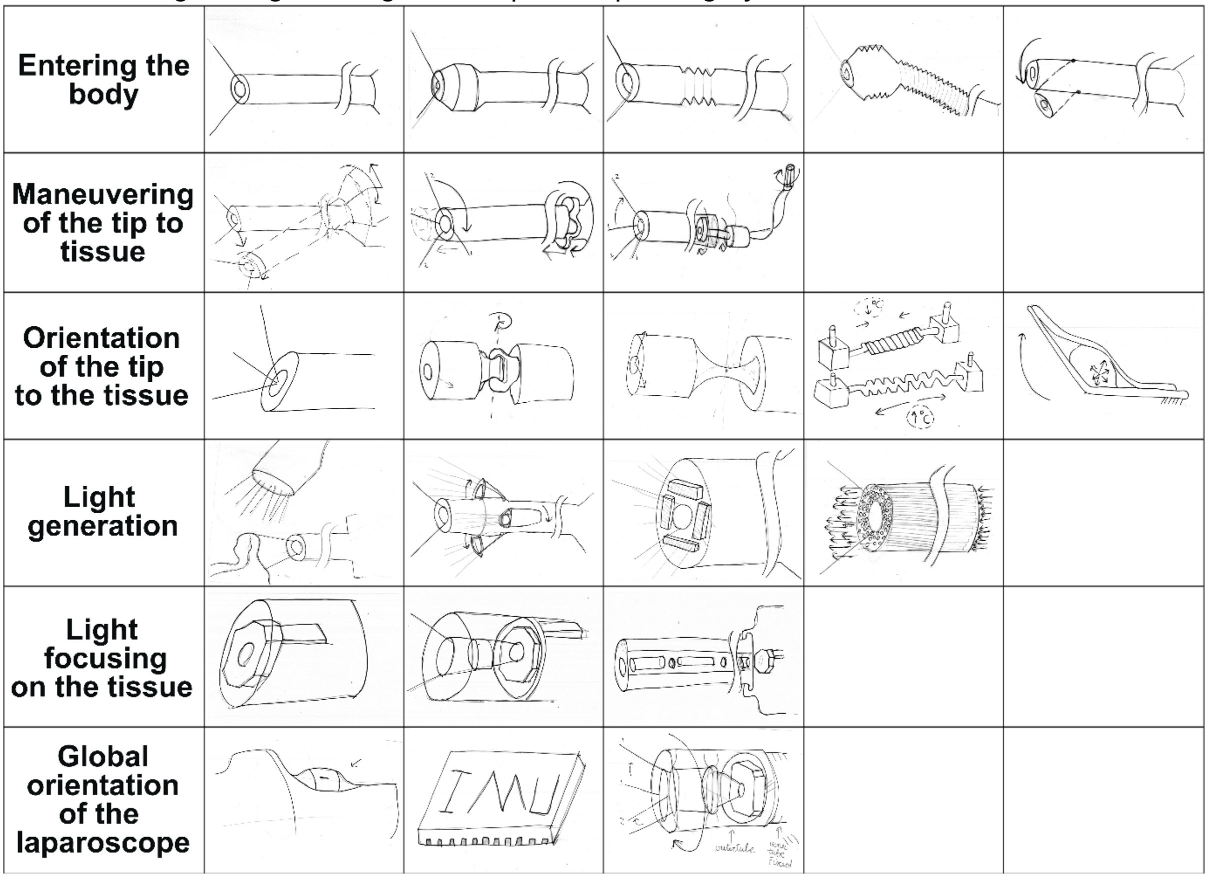

Figure A: morphological chart of the functions and their design solutions.

Appendix 2.2: Morphological overview discarding explanation

The solution in the morphological chart(appendix 2.1) had to be considered to design the most promising designs, and the design options that would result in the breaching of functional requirements were discarded. In maneuvering the tip-to-tissue function, the last option regarding control utilizing electrical actuators is not included in one of the six concepts because this solution would increase the initial purchasing cost of the device over the set requirement. In orienting the tip to the tissue at the required angle, the last two options are not included with the same reasoning as the actuator in the previous function, cost. The shape memory alloy often used in endoscopes for the bending sections is made of nitinol filaments. A current is applied to heat the nitinol filament and change the material's properties to extend or contract. The use of this technique would require sophisticated components and control. The microfluidic mechanism would require a pump to inflate and deflate the bending section. Lastly, the light emitting shaft was not included based on the increased complexity and, therefore, the disinfection compatibility with the reprocessing, which could damage the device when cleaned or sterilized or HLD.

Appendix 2.3: Concept Performance Scores Explanation

In order to converge on a final design, the concepts are scored based on the performance criteria, which are all weighted based on the importance noted by surgeons and literature, as found in Table 1.

Cost: The cost is based on the required components to construct the concepts. If the costs are under 100 euros in parts, the design gets awarded 5 points, and a cost of 300 euros gets awarded 1 point.

- Concept 1: Eliminates the need for the processor and light source but still requires a short optical fiber to connect the camera head to the slender scope. The assumption is made that these lenses are already available and do not play a part in the cost, but the customized optical fiber will result in a score of 1.
- Concept 2: It employs a simple design without any complicated components and would not need much more than a small USB to LED transformer, imaging systems LEDs, a medical steel shaft, and a handle, which would cost less than 100 euros.
- Concept 3: it requires the same components as Concept 2, with the addition of some optical components, an outer tube, and seals. Adding optical components will increase the price significantly, resulting in a score of 2.
- Concept 4: Again, it shares the same components as Concept 2 with additional parts for the bending movement, such as Nitinol wire, flexible shrink wrap, cables, and small plastic components. These components are not expensive since the bending section is 3cm long, resulting in a score of 4.
- Concept 5: As with Concept 4, additional parts are required for the bending motion of the tip. Here, components such as a torsion spring, small plastic components, and flexible heat shrink are necessary, resulting in a score of 4.
- Concept 6: The final concept shares the same components as concept 2 with the difference of having a different tip, which requires a small extra component and still results in a score of 5.

Invasiveness: The invasiveness is based on the diameter of the scope shaft. When smaller or equal to 10mm, a score of 5 is awarded; when up to 15 mm, a score of 1 is awarded.
● Concept 1: The first concept uses a standard slender lens, making using 5mm and larger scopes possible, resulting in a score of 5.
● Concept 2: The second concept orients the image sensor at the tip at 30 degrees. The minimum diameter required for this sensor at this orientation is 12.5mm without a shaft, resulting in an estimated diameter of around 14mm and a score of 2.
● Concept 3: The idea uses two outer shafts with a thickness of 0.5mm over top of each other, with the sensor placed straight in the shaft requiring about 13 mm, resulting in a radius of about 15mm and a score of 1.
● Concept 4: Uses the lower height of the sensors and places it flat with a 90-degree offset from the tip direction, which is bent to be oriented at 30 degrees. The orientation of the sensors makes it possible to fit the sensor in an 11mm shaft with 0.5mm wall thickness, resulting in a score of 4.
● Concept 5: Employs a similar concept where the sensor is oriented at 60 degrees and rotated 30 degrees back to the required orientation. The outer diameter with a shaft of 0.5mm would result in about 12mm and a score of 3.
● Concept 6: It uses a beveled tip, which needs to be 15mm, which would result in a score of 1.

Robustness: The robustness of a design is required for this use case. The design without any brittle components will be awarded a score of 5, and a design with many brittle components will be awarded a score of 1.
● Concept 1: Uses a slender scope consisting of a large set of brittle Hopkins lenses, resulting in a score of 1.
● Concept 2: Uses no glass except in the cover, shielding the LEDs and the camera from the outside world. The image sensor lenses consisted of plastics, making the glass plate the only brittle component used, resulting in a score of 4.
● Concept 3: Utilizes a set of lenses to focus the light at the image sensor and to shield the ends of both shafts. The use of some optical components results in more brittle components and a score of 2.
● Concepts 4,5,6: Just as Concept 2 only uses an end plate to close the image sensor and the LEDs off from the outside world, and therefore scores a 4 as well.

Ease of reprocess ability: The ability to clean and disinfect the scope is essential. The fewer steps that need to be taken will reduce the change of errors in the reprocessing. If a design considers one solid part not requiring disassembly, then it is awarded a score of 5, and when sub-assemblies have to be dismantled, a score of 1 is awarded.
● Concept 1: Consists of two major parts: the Hopkins lens and the camera head with the c-mount. These two components can easily be reprocessed with any further disassembly but need to be checked to be put together again. Also, the c-mount needs to be inspected, resulting in a score of 3.
● Concept 2,6: Consists of only one part and therefore needs to disassemble no further, resulting in a score of 5.
● Concept 3: Utilizes two shafts rotating over each other, which is sealed with a piston rod seal. The seal should be able to keep all liquids out but needs to be checked, resulting in a score of 3.
● Concepts 4,5: the concepts are all made out of one part, which is sealed with shrink wrap and needs to be inspected, resulting in a score of for both of them is 4.

Serviceability: The device should be able to be repaired when a component breaks. If the device can be repaired locally without requiring specific tools, the design is awarded a score of 5. If the device is not repairable and needs to be replaced when broken, a score of 1 is awarded.

● Concept 1: the design consists of the head and the scope. Based on the serviceability of the scope alone, the design scores a 1.

● Concept 2, 6: have a fully closed design where the electronics could be recovered in the handle, but the rest of the device would need to be replaced, resulting in a score of 2.

● Concept 3: Utilize the two shafts over top of each other, which could be replaced separately from each other, and another outer shaft could be used with different optics for different orientations, resulting in some modularity and a score of 3.

● Concept 4,5: both use bending sections with the image sensor at the end, which could be replaced if the LEDs or image sensor breaks. As with Concept 2, the electronic can be salvaged, resulting in a score of 3

Compatibility: If the Design can be used with readily available instruments, the design is awarded a score of 5. When it requires uncommon or specific equipment to be used, a score of 1 is awarded.

● Concept 1: It uses the standard scope attachment and is therefore compatible with standard equipment used worldwide, resulting in a score of 5.

● Concepts 2,3: These concepts need to use a nonstandard 15mm trocar for gas laparoscopy, resulting in a score of 2.

● Concept 4,5: The concept would not be able to be used with 10mm trocars but would require 12mm trocars, which are still readily available, resulting in a score of 4.

● Concept 6: The alternative method of entering by stretching would require specific flexible inside trocars, requiring specific equipment, resulting in a score of 1.

Based on the functional and performance requirements for designing a laparoscope for low-income settings in India and sub-Saharan Africa, it was found, based on the Harris profile as shown in Table 4, that concepts 4 and 5 are the most promising concepts. These concepts will be prototyped to validate the effectiveness and optimize the design.

Appendix 2.4: Intermediate prototype testing

The initial prototypes were tested, and the demonstrational videos were recorded with multiple views. The videos show the actuation of concept 4 and the problem of getting the shaft straight. The use of Resolume Avenue is also demonstrated, showing multiple camera views at ones on one screen. The videos can be found on my YouTube channel created for this project at: https://www.youtube.com/@rafaelvanloon9165

Appendix 2.5: bending section experiments

The initial design of the bending section for the FlexEye concept experienced problems that made it impossible to straighten the shaft to make it pass through a trocar. That would mean the concept does not comply with the functional requirements. The reason was narrowed down to friction and slack of the single cable used. In order to validate these hypotheses, a larger scale model was built to test how to solve the problems experienced for the final design, with the additional goal of seeing if some mechanism that would fit in the handle would make it possible to balance the bending sections statically.

Options such as crossing the wires inside the handle solved the problem that the length of the wire was the same in all configurations of the bending sections, though this resulted in non-balanced forces. If the wires were not crossed and the bedding section was bent at the same angle, the forces would be balanced, but though the nature of that, the internal section of a bending beam gets compressed, which means for the bending sections, the case the length of the cable is shortened was not able to be set at a different angle as the angle in which the cable where tightened.

Experiments relating to keeping the length of the cable constant by using spring-based mechanisms, such as illustrated in Figure B, and fiction-based mechanisms for the crossed wires showed some positive results. Still, fears relating to the complexity and wear of the cable through friction resulted in dropping the static balancing mechanism. Through this prototype, it was found that using two wires at both ends of the end section of the bending section resolved the problems relating to slack, and using bigger holes in the bending section parts resolved the friction problems, which resulted in the bending section design of the final FlexMod design for the gas laparoscope.

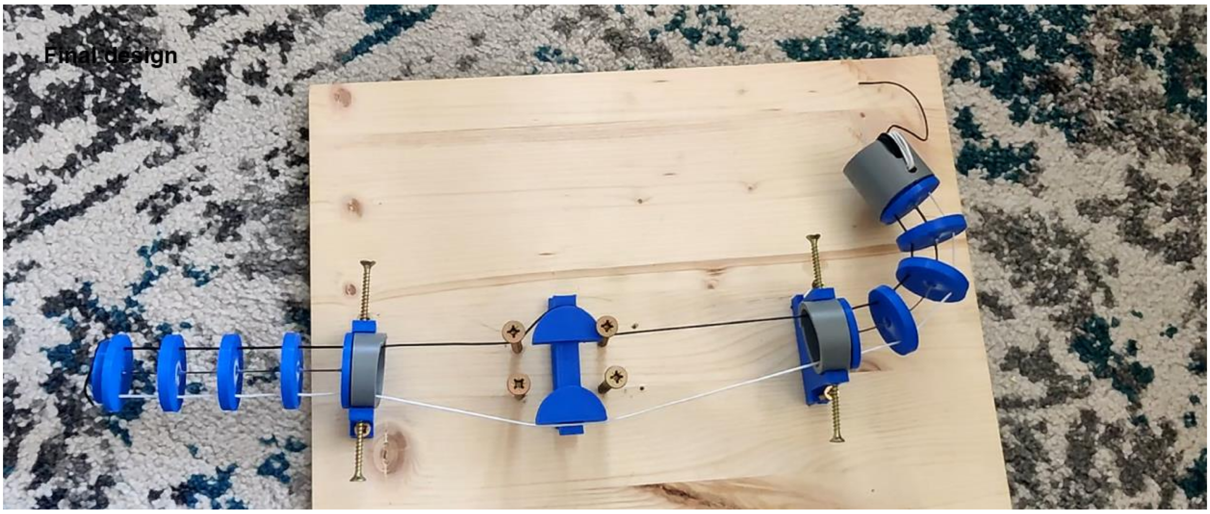

Figure B: Test setup for the development of the bending section of the FLexEye concept.

Appendix 2.6: Customized imaging system for the FlexMod Laparoscope

The standard length of the imaging system cable was only 180mm, which makes it impossible to create a laparoscope that fore fills the functional requirements stating that the tip that enters the body should be 300 mm from the handle to be able to reach all places in the abdomen from the same entry hole. To address this issue, agreements with the imaging systems producer were made to proof the version of the image systems with a cable length of 300mm, for which the production drawings are listed in Figure C. The new imaging system configuration allows the creation of a laparoscope with the required shaft length. The contracted vendor is the same as noted for the imaging system in Appendix 1.1.

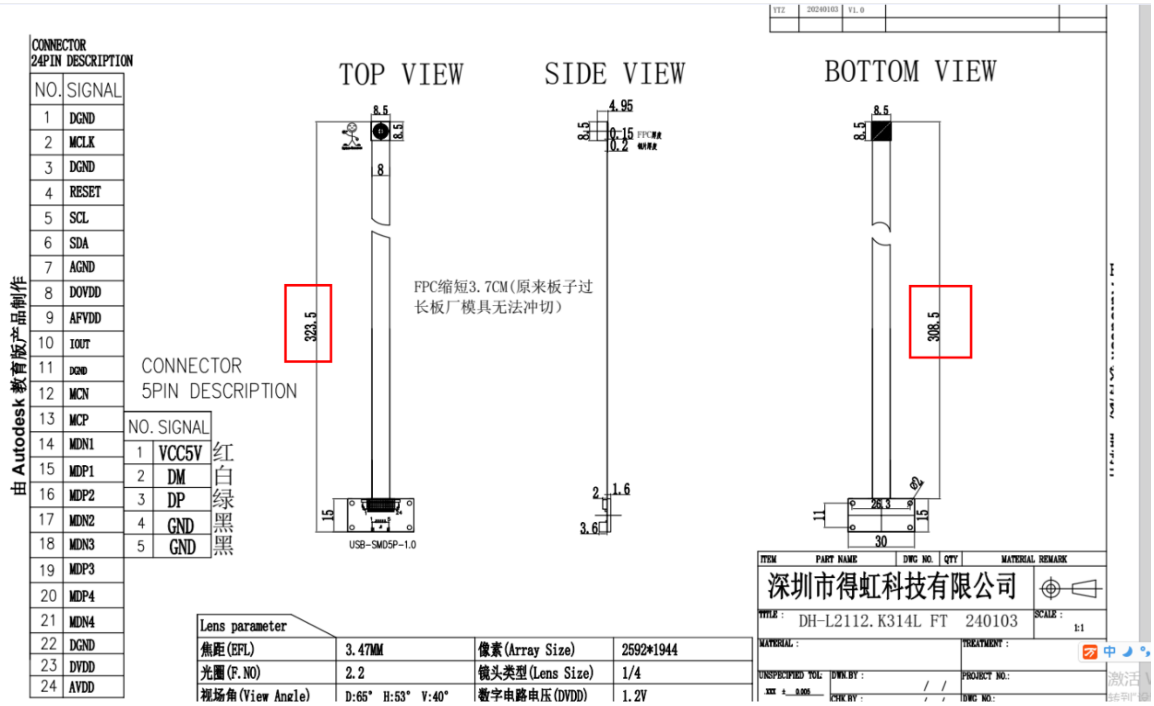

Figure C: Construction drawing for the customized imaging system, with increased ribbon cable length as highlighted in red.

Appendix 2.7: Expanded price overview of both types of laparoscopes

A complete overview of all the costs relating to the required components for the construction of both types of laparoscopes is given in Table A. The list shows that most components between the gas and gasless designs are the same, resulting in a similar price. The table does not include the imaging software, which has been advised, though this software is not necessary to use the device.

Table A: The complete list of required components and their associated costs.

	Gas 1	Gas 50>	Gasless 1	Gasless 50>
Custom OmniVision 5693-based imaging system	88.00	38.00	88.00	38.00
LEDs(5730, 6000k LED) and Circuit	1.35	1.35	1.35	1.35
Transformer(5v to 3.3v)	2.34	1.28	2.34	1.28
Isolated electrical wires 1M	0.07	0.07	0.07	0.07
Medical heat shrink (TE connectivity 10-12mm tube)	0.1m = 5.74	0.1m = 5.17	0m = 0.00	0m = 0.00
10mm od, 0.5mm wall, 300mm length, 316l stainless steel	11.48	7.65	11.48	7.65
2 x (m4 bolt of 40mm)	0.47	0.47	0.47	0.47
1 x (m4 bolt of 20mm)	0.15	0.15	0.15	0.15
50 ohm, 150 ohm, breadboard	0.93	0.93	0.93	0.93
Epoxy glue	1.00	1.00	1.00	1.00
ABS handle (120g)	2.76	2.76	2.76	2.76
Additional ABS parts	0.80	0.80	0.11	0.11
Additional non-3D-printed parts	1.41	1.41	0.00	0.00
1mm by 1mm silicone strip as gasket	0.13	0.13	0.13	0.13
2-meter shielded USB 2.0 cable	7.09	6.24	7.09	6.24
1.5m of 1mm 304 stainless cable	0.31	0.31	0.00	0.00
Grillamid lens cover	1.00	1.00	1.00	1.00
Total	124.96	68.72	116.88	67.09

Appendix 2.8: Future design input and most recent prototype

Future design improvements will be based on the findings of the final gasless prototype and the second round of user feedback from a laparoscopic surgeon. The ideas proposed by Dr. J. Gnanaraj were related to SILS by reducing the shaft size to create more space for instruments in the same entry point. The design iteration will no longer use a round shaft but a bent beam of 10 mm by 2mm, as shown in Figure D. The image sensor's ribbon cable and the LEDs' power cables will be run over the shaft and sealed using a medical heat shrink. The tip does not have to be round and will have a rounded rectangular shape that houses the LEDs and image sensor, which are separated to eliminate the effects of the lens glare. So that the materials now at hand which are validated for use with the sterilizing agents, can be used to bring the scope quicker to those who need it.

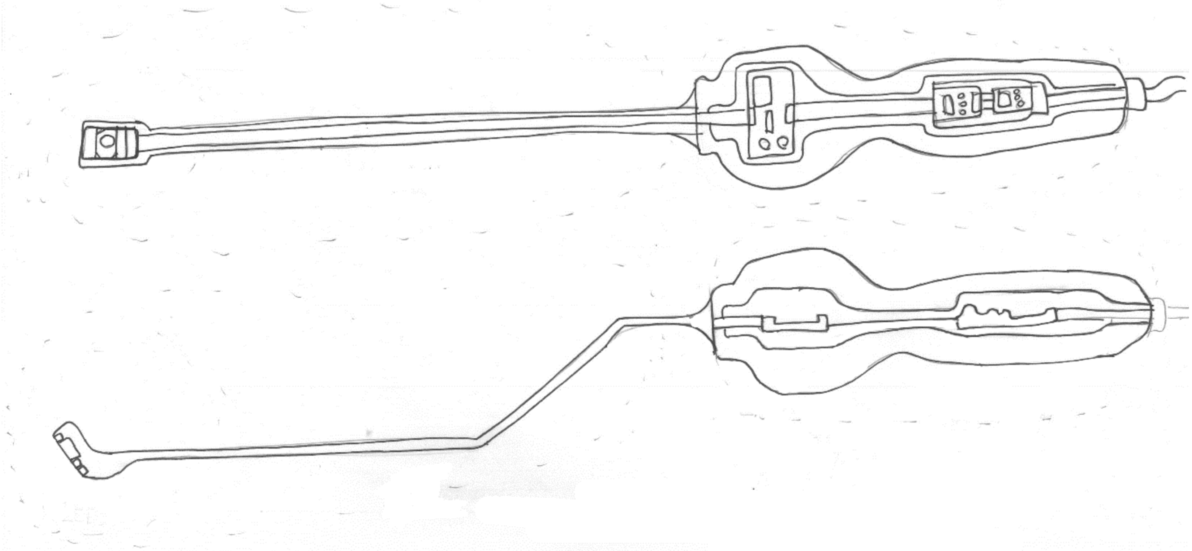

Figure D: Beam shaft gasless laparoscope.

This device version is already designed but was not fully completed and, therefore, not included in the final design section of the second part of this thesis. This version of the laparoscope is expected to be ready in February 2024. The components produced for this prototype are shown in Figure E. All required parts are sourced, and only minor ABS components need to be produced before a new prototype can be finished.

Figure E: Components produced for the updated gasless laparoscope.